Canadian Geotechnical Journal

OPEN ACCESS | Research Article

Practical guidelines on the determination of one-dimensional swell properties of highly expansive clays

R.A. Murison[a], **T.A.V. Gaspar**[b], **S.W. Jacobsz**[a], **G. Heymann**[a], **and A.S. Osman**[c]

[a]Department of Civil Engineering, University of Pretoria, South Africa; [b]Department of Civil & Environmental Engineering, Imperial College London, United Kingdom; [c]Department of Engineering, Durham University, United Kingdom

Corresponding author: **R.A. Murison** (email: ruan.murison@tuks.co.za)

Abstract

Engineers typically require two parameters for the understanding of expansive soils to limit damages invoked by volume change: the swell pressure – the stress required to completely restrain volume change upon inundation – and the swell potential – the volume increase exhibited upon inundation at a given stress level. These properties have been shown to be dependent on the stress path followed during their measurement in the laboratory. This creates challenges for practitioners attempting to obtain reliable swell properties without an extensive testing programme. A discussion of the stress path-dependency and reasons for variations of the measured swell properties within a Barcelona Extended Model (BExM) framework is given. Series of oedometer tests following three standard methods for the determination of swell pressure and swell potential were carried out for two highly expansive clay soils with different microfabric types. After swell phases, samples were consolidated to high stresses (up to 4 MPa). For both soils, the magnitudes of the swell properties relative to one another, when measured using the different experimental methods, aligned with the predicted hierarchy according to the theoretical framework. This verifies the suitability of the framework for both microfabric types. The insights gained from the test results and theoretical framework were used to design a minimum testing programme for practitioners, allowing robust determination of the swell pressure and swell potential of a given clay.

Key words: expansive clays, oedometer testing, unsaturated soils, swell pressure, swell potential, microfabric

Résumé

Les ingénieurs ont généralement besoin de deux paramètres pour comprendre les sols expansifs afin de limiter les dommages causés par le changement de volume : la pression de gonflement – la contrainte requise pour limiter complètement le changement de volume lors de l'inondation – et le potentiel de gonflement – l'augmentation de volume présentée lors de l'inondation à un niveau de contrainte donné. Il a été démontré que ces propriétés dépendent du trajet de contrainte suivi lors de leur mesure en laboratoire. Cela crée des défis pour les praticiens afin d'obtenir des propriétés de gonflement fiables sans un programme de tests approfondi. Une discussion sur la dépendance au trajet de contrainte et les raisons des variations des propriétés de gonflement mesurées dans le cadre du modèle étendu de Barcelone (BExM) est présentée. Une série de tests d'oedomètre suivant trois méthodes standard pour la détermination de la pression de gonflement et du potentiel de gonflement a été réalisée sur deux sols argileux hautement expansifs de types de microfabrique différents. Après les phases de gonflement, les échantillons ont été consolidés sous des contraintes élevées (jusqu'à 4 MPa). Pour les deux sols, les magnitudes des propriétés de gonflement mesurées expérimentalement, par rapport les unes aux autres à l'aide des différentes méthodes, ont été conformes à la hiérarchie prédite selon le cadre théorique. Cela vérie l'adéquation du cadre pour les deux types de microfabrique. Ces connaissances ont été utilisés pour concevoir un programme d'essais minimal pour les praticiens, afin de déterminer de manière robuste la pression de gonflement et le potentiel de gonflement d'une argile donnée.

Mots-clés : argiles expansives, essais oedométriques, sols non saturés, pression de gonflement, potentiel de gonflement, microfabrique

1. Introduction

Expansive (or "swelling") clays are problem soils which exhibit large volume changes due to variations in water content. The seasonal wetting and drying of these soils may lead to significant swelling and shrinkage, causing distress to infrastructure founded on or within a profile contain-

ing the active expansive clay strata. In the USA, the annual cost associated with structural damage caused by expansive soils has been quoted to substantially exceed the combined cost of all other natural disasters, such as earthquakes and hurricanes (e.g., Jones and Holtz 1973; Nelson and Miller 1992).

All unsaturated soils have the potential to exhibit some volume change with variations in water content, due to alterations in particle contact forces brought about by the associated changes in soil suction. There are two particular factors that set expansive clays apart from other clays and unsaturated soils. The first is that hydration can occur within the clay lattice of expansive soils due to their mineralogy, which is typically primarily constituted of smectite group minerals such as montmorillonite. Stronger bonds between platelets of other phyllosilicate clay minerals, such as illite and kaolinite, generally only allow for hydration at the edges of clay lattices. For this reason, far greater volume changes can be induced in expansive soils due to hydration. The second characteristic factor is that large plastic (irrecoverable) volume changes may occur upon wetting of expansive soils (Gens and Alonso 1992), as opposed to exclusively elastic changes in most other unsaturated soils (excluding collapsible soils). This provides additional challenges in the modelling and general understanding of the swelling behaviour of expansive clays. Gens and Alonso (1992) showed that it is useful to separately consider microstructural and macrostructural components of swell, but that the two structural levels are coupled. Experimental quantification of the magnitude of microstructural swell requires sophisticated equipment (Lourenço et al. 2008; Romero and Simms 2008) and was not considered in this study. However, even a conceptual consideration of the microfabric of expansive clays can provide useful insights into understanding the macroscopic behaviour. Conventional laboratory methods are targeted toward the measurement of macrostructural behaviour, which is ultimately what is of interest to the geopractitioner.

Despite the advancement in knowledge surrounding expansive clays, routine testing procedures have remained relatively unchanged over the years. With the introduction of suction-controlled oedometers, it is now possible to perform sophisticated testing of swelling clays that can produce substantially more information on the behaviour of this problem soil. However, such testing has been largely confined to the research community, since few institutions across the world possess the necessary testing equipment. Furthermore, the time and cost associated with such testing makes it unfeasible for routine use in industry.

It is therefore useful to revisit and evaluate conventional oedometer testing for expansive clays, using the insights gained from more sophisticated testing. This paper first outlines the various conventional oedometer testing procedures routinely employed by practitioners to characterise key swell properties. Thereafter, the results of a suite of oedometer tests on two highly expansive clays from South Africa are reported. The rationale for selecting the two clays considered is that they represent two distinct fabric types which are typical for expansive clays. The differences in results between the testing methods, and the behaviour of the two clays, are interpreted with reference to microfabric observed using scanning electron microscopy. Such considerations of the microfabric have allowed interpretation of results within the framework of the Barcelona Extended Model (BExM) for highly expansive soils (Gens and Alonso 1992).

Although previous studies have noted differences in swell properties between the different standard test methods, guidelines on what tests are required for robust determination of these properties have not been explicitly outlined. The results of the current study and the evidence from the BExM framework have been used for the first time to propose a novel testing programme independent of fabric, which allows practitioners to obtain reliable and conservative swell properties for any construction sequence using a minimum of three conventional tests. The programme also allows for confident determination of saturated consolidation properties, and identification of temporal swelling phenomena for the given clay.

2. Oedometer test methods for expansive clays

Oedometer testing of expansive clays is generally used to assess two parameters of importance:

- The magnitude of pressure required to completely prevent swell, referred to as the *swell pressure*.
- The magnitude of swell that can be expected under various overburden stresses, referred to as the *swell potential*.

Of the conventional oedometer tests readily available to geotechnical practitioners, all suffer from the drawback of reducing a sample to a point of zero suction (sometimes erroneously interpreted as full saturation) (Schreiner 1988). While this condition is generally assumed as unlikely to occur in practice, useful information can still be obtained from these tests if their limitations are understood, and their relevant applications borne in mind. A summary of conventional approaches is provided in Table 1, along with the typical construction sequence emulated by the stress path followed in each test method. Brief explanations of the various tests are provided in the subsequent sections.

2.1. Double oedometer test

Jennings and Knight (1957) proposed a method for determining the swell potential of expansive clays, or the collapse potential of collapsible soils, using parallel samples in two oedometers. Two samples are prepared in an unsaturated state at their in-situ water content and density. One sample is sealed to prevent any change in water content and tested in an unsaturated state. Loads are incrementally applied and the change in volume associated with each increment is recorded. The other sample is inundated with water under a small seating stress and allowed to swell to a state of zero suction. After the swelling stage is complete,

Table 1. Oedometer test methods for expansive clays.

Test name	Example of typical construction sequence for which the test stress path is relevant (after Schreiner and Burland 1991)
Double oedometer test (Jennings and Knight 1957)	Soil profile is wetted prior to construction
Loading after wetting (ASTM D4546-21) Also referred to as: • swell followed by consolidation (Schreiner 1988) • single oedometer test (Jennings et al. 1973*a*)	Soil profile is wetted prior to construction
Wetting after loading (ASTM D4546-21) Also referred to as: • swell under constant stress (Holtz and Gibbs 1956; Schreiner et al. 1994)	Changes in moisture content occur after the structure has been built
Constant volume swell (BS 1377-5:1990*; Sullivan and McClelland 1969)	Not representative of any typical construction sequence

*Clauses 4.3 and 4.4.

Fig. 1. Determination of swell potential using the double oedometer test (after Jennings and Knight 1957).

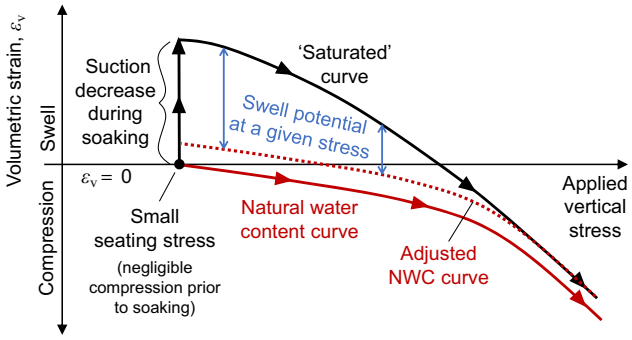

Fig. 2. Determination of swell potential and swell pressure using a loading after wetting test.

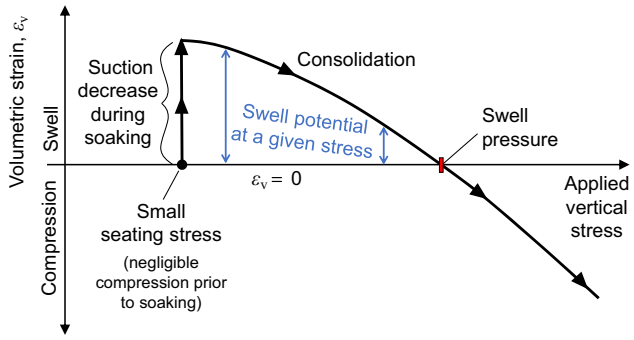

the sample is incrementally consolidated in the conventional manner. This was termed the "saturated" test by Jennings and Knight (1957), although of course full saturation cannot be confirmed in conventional oedometers. Jennings and Knight (1957) suggested that the loading curve of the natural water content test should be adjusted such that the curves of the two tests coincide once they begin to run parallel. The offset between the "saturated" and adjusted curve is the swell potential at any given stress level. The definition of swell potential using the test method is given in Fig. 1. Jennings and Kerrich (1962) discussed how the assumption that the two curves should coincide only applies if the traditional law of effective stress holds true for the given initial state of the unsaturated soil. This method is thus applicable only for a narrow upper range of initial degrees of saturation.

2.2. Loading after wetting

This test procedure was derived from the double oedometer test, but only one sample is tested. Several variations of this test have been described in the literature (e.g., Jennings et al. 1973*a*; Sridharan et al. 1986). The sample is prepared and placed in the oedometer at its in-situ state (i.e., void ratio and water content). As with the "saturated" sample in the double oedometer test, a small seating stress is applied to the sample in its unsaturated state. The cell is then filled with water, allowing the sample to swell. After the sample has been brought to a state of zero suction, consolidation stages are applied. In this case, the swell potential is defined as the volumetric strain on the loading path at the stress of interest, and the swell pressure is the stress at which the consolidation curve has intersected the initial void ratio (i.e., the stress at which the sample is consolidated back to zero volumetric strain). The concept of the test is illustrated in Fig. 2. Different magnitudes for the nominal seating stress have been recommended in the literature, such as 1 kPa in a study by Jennings and Knight (1957), and 6 kPa in a study by Sridharan et al. (1986). A standard test method that can be followed to carry out the test is the "loading after wetting" procedure in ASTM D4546-21.

2.3. Wetting after loading

Holtz and Gibbs (1956) proposed a test method to directly measure swell potential under a given stress. As with the previous methods, a sample is prepared at its in-situ water content and void ratio. A seating stress corresponding with the expected in-situ stress (for example, overburden stress plus an expected foundation load) is applied to the sample in its unsaturated state. After applying the desired net vertical stress (termed the "soaking stress"), the cell is inundated

Fig. 3. Determination of swell potential and swell pressure using (*a*) a single wetting after loading test; (*b*) series of swell tests under various constant loads (soaking-under-load curve method).

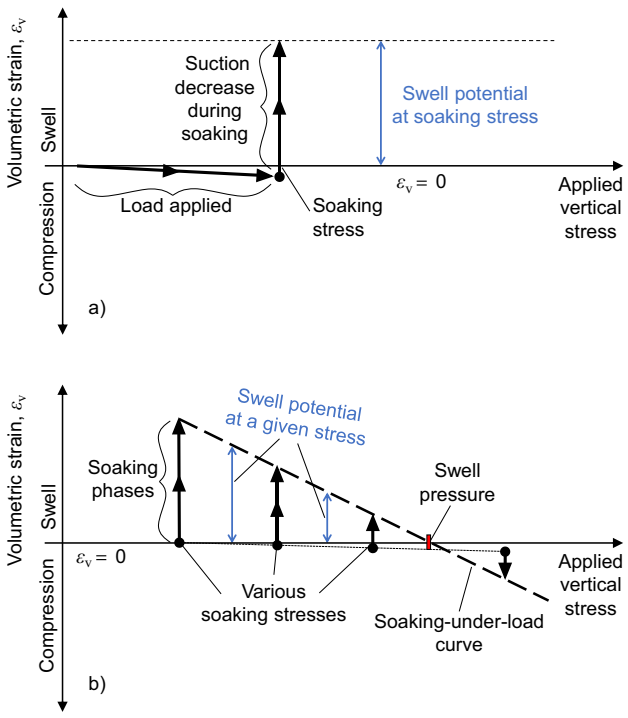

with water and the sample is allowed to swell/compress vertically as the suction is reduced to zero. The vertical strain achieved once the sample has reached equilibrium is the swell potential at the given stress. The stress path followed is illustrated in Fig. 3*a*. If a series of these tests is performed under various constant soaking stresses, the swell pressure may be determined. Connecting the equilibrium points after soaking under various stresses defines what is known as a "soaking-under-load" curve. The swell potential at any given stress may be read off from this curve, and the intersection of the soaking-under-load curve with zero volumetric strain is the swell pressure. This is illustrated in Fig. 3*b*. Note that some compression would likely occur during loading of the unsaturated sample, but this volume change is generally small relative to the magnitude of swell during soaking. A standard test method that can be followed to carry out these tests is the "wetting after loading" test procedure in ASTM D4546-21.

2.4. Constant volume soaking

A direct measure of swell pressure using a single test may be achieved by maintaining a constant sample volume during soaking, and recording the stress required to impose this condition as the suction is reduced to zero. This is difficult to achieve using a conventional oedometer apparatus, as it requires constant monitoring of displacement and a manual change in applied stresses in response to any change in the displacement reading. Of course, the smaller the increments of strain that are induced before increasing the load to suppress swell, the closer one is to measuring a true constant volume stress path. The magnitude of the swell pressure measured using this technique has been observed to be sensitive to any volume change taking place during soaking, causing undermeasurement. As a result, Fredlund et al. (1980) suggested a graphical correction to the swell pressure path by subtracting the system flexibility, measured by replacing the oedometer sample with a steel disc. Further empirical graphical constructions proposed by Fredlund et al. (1980) or Nelson and Miller (1992) can be applied to correct for sampling disturbance if intact (or "undisturbed") samples are being tested.

Fig. 4. Determination of swell pressure from constant volume soaking and swell potential from unloading (after Sullivan and McClelland 1969).

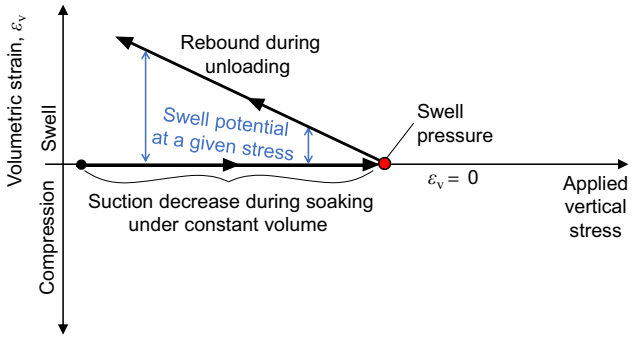

The constant volume soaking process can be automated using modern automatic oedometer frames with a feedback loop between the force and displacement transducers. Sullivan and McClelland (1969) suggested that if the sample is unloaded in the conventional manner after the constant volume soaking phase, the swell potential can be estimated from the rebound curve. The stress path followed during the test is illustrated in Fig. 4. This swell potential prediction only captures elastic deformation – a shortcoming which is discussed in Section 3.

Alpan (1957) and Brackley (1973) each developed test methods aiming to determine the constant volume swell pressure, by enforcing constant volume conditions using a stiff frame and measuring the swell pressure that developed using a stiff load cell or proving ring. The load cell and frame should be sufficiently stiff such that any change in volume of the sample due to deflection of the system is negligible. Similar approaches have been used in recent publications (e.g., Manca et al. 2016).

As mentioned, an automatic oedometer can also be utilised for this test. An advantage of the automatic oedometer is that true constant volume conditions can be maintained by adjusting the pedestal to counter any small deflections of the load cell, using a feedback loop that maintains a constant displacement transducer reading. In addition, once the sample has been brought to a state of zero suction, the volumetric strain can be tracked as the sample is unloaded to known stresses. This is achieved by recording the resulting displacement transducer reading whilst continuously adjusting the

pedestal such that a constant force is maintained for each unloading increment. A standard test method for constant volume soaking followed by unloading is outlined in Clauses 4.3 and 4.4 in BS 1377-5:1990.

2.5. Suction-controlled testing

Recent advancements in laboratory testing have allowed for the control of suction in the oedometer, allowing the previously discussed stress paths to be imposed in a more controlled manner, and without the need for full sample inundation. The three main types of suction control typically utilised include axis-translation, osmotic control, and vapour equilibrium, which target the low, medium, and high suction ranges, respectively.

The axis-translation technique, first proposed by Hilf (1956), involves artificially increasing the pore air pressure (u_a), such that control of a positive pore water pressure (u_w) allows for a positive matric suction ($u_a - u_w$) to be imposed. The method has been applied in suction-controlled oedometer testing in studies by Schreiner and Burland (1991), Schreiner et al. (1994), and Bagheri et al. (2020). The approach is typically quoted as having an upper suction limit of 1500 kPa, which is governed by the high-air entry disc used and the maximum capacity of the pressurised air supply system (Bagheri et al. 2020). In addition to the limited measurement range, a criticism of the method is that elevated air pressure may cause irreversible changes to the soil fabric if the pore air phase is not continuous, in which case it imposes a total stress on the soil skeleton (Delage et al. 2008).

Osmotic suction control involves enclosing the sample in a semi-permeable membrane (permeable to water but not salts) and circulating a polyethylene glycol (PEG) solution behind the membrane. The method was first introduced to geotechnical engineering in the form of a suction-controlled oedometer by Kassiff and Ben Shalom (1971). The osmotic technique imposes a matric suction to the soil, which increases with increasing PEG concentration. An advantage of the method over axis-translation is that a more realistic suction condition is imposed on the sample, i.e., without imposing an artificial air pressure (Delage and Cui 2008). Furthermore, while the approach does have a theoretically higher suction range than the axis-translation technique of up to 10 MPa (Delage et al. 1998), it does require calibrations to relate imposed suctions to PEG concentration. As a result, the practical range of the approach is limited by the measurement capacity of the instrument used to calibrate it. Various calibrations reported in the literature (Dineen and Burland 1995; Tarantino and Mongiovi 2000; Monroy et al. 2007) have also highlighted how the calibration is dependent on both the membrane type and nature of the PEG used (Delage and Cui 2008). Perhaps the greatest shortcoming and challenge of the approach is degradation of cellulotic semi-permeable membranes due to mechanical shearing and bacterial attack. While some studies have illustrated successful imposition of suction for up to 146 days without issues when using synthetic membranes (Monroy et al. 2007, 2015), expansive clay tests often take significantly longer (as was the case for many of the tests in the current study) making the osmotic approach problematic.

For suction control in the high-megapascal range, the vapour equilibrium technique with relative humidity control can be utilised. By controlling relative humidity and temperature, and allowing equilibrium to occur through exchange of water through the vapour phase, a known total suction (governed by Kelvin's law (Thompson 1871)) is imposed on the soil sample. Example uses of the vapour equilibrium technique include Likos and Lu (2003), who measured soil-water retention curves between suctions of 7–700 MPa, and Mantikos (2018), who developed a modified oedometer capable of imposing suctions of up to 100 MPa. Whilst the method is useful at very high suctions, a shortcoming of the method is that the imposed suction is extremely sensitive to changes in relative humidity. Likos and Lu (2003) reported a maximum deviation in relative humidity of 0.6% in their apparatus. While seemingly small, this variation resulted in suction variations of approximately 1 MPa in the 7–10 MPa range. Mantikos (2018) reported a suction uncertainty of approximately 1.7 MPa in the same range. For soils where suctions are typically in the range of 1–10 MPa, such as those tested in the current study, such variations would substantially influence the mechanical response.

Considering the limitations of the discussed approaches, it can be seen that they would all be limited in their ability to control suction in the ranges under consideration for this study (1–10 MPa), and are likely to present challenges for the longer testing times required. Furthermore, as previously stated, only a few academic institutions have access to suction-controlled oedometers making their routine use in industry unfeasible. As a result, this study aims to develop guidelines that can be implemented in conventional oedometer testing which is available in most commercial laboratories.

3. Stress path-dependency according to the BExM

Each of the discussed methods considers a different stress path to determine both swell potential and swell pressure. Experimental investigations have shown variations in the measured properties, depending on the stress path followed (e.g., Brackley 1975; Justo et al. 1984; Sridharan et al. 1986; Monroy et al. 2015).

The reasons behind the differences in measured swell pressure and swell potential for the various methods, and the dependency of these parameters on the stress path followed during testing, can be better understood by considering the tests in a conceptual unsaturated critical state soil mechanics framework. The BExM for highly expansive clays (Gens and Alonso 1992) was used for this purpose. Figure 5 shows expected stress paths according to the BExM in suction (s) vs net mean stress ($\bar{p}$) and void ratio (e) vs net mean stress planes for hypothetical samples subjected to various test methods. An identical initial state, given by (e_0, s_0, $\bar{p}_0$) applies to each hypothetical test. A *loading after wetting* test for a sample soaked under a constant nominal seating net stress is given by Path A

Fig. 5. Yield loci and state paths in loading after wetting, wetting after loading, and constant suction tests in the BExM framework (after Gens and Alonso 1992).

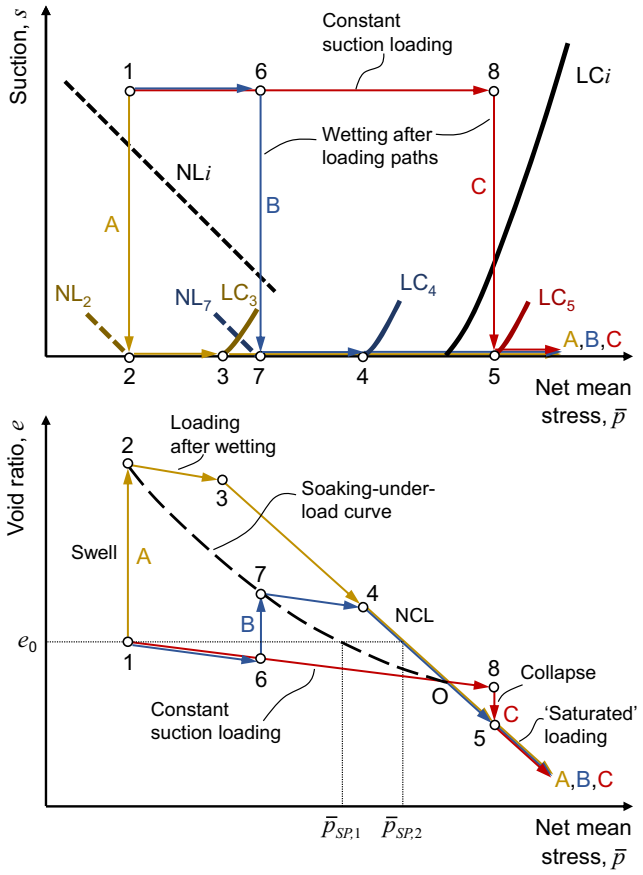

(1-2-3-4-5). *Wetting after loading* tests are given by Path B (1-6-7-4-5) for a sample soaked at a constant stress significantly less than the swell pressure, and by Path C (1-6-8-5) for a sample soaked at a stress greater than the swell pressure. The pre-wetting phases of Path C (1-6-8) also represent the *constant suction* loading path, i.e., the slope of this path in the e-log$\bar{p}$ plane would represent the compressibility of a soil element in its natural unsaturated state that is only subjected to changes in mechanical stress. The "saturated" normal consolidation line (NCL), given by Path 3-4-5, is assumed to be unique. Positions of the neutral loading (NL) lines, which serve a purpose similar to yield loci on the microstructural scale, as well as the load–collapse (LC) yield curves, which represent yield loci on a macrostructural scale, are indicated at various key points along these stress paths in Fig. 5. The supplementary material to this article gives a detailed description of the generation of these stress paths according to the BExM model (Gens and Alonso 1992) using the positions of the NL and LC loci, the soaking-under-load curve, and the concept of macrostructural softening induced by microstructural strain.

Given the assumptions made by the BExM and in the constructions of the stress paths outlined in Fig. 5, a number of consequences regarding the swell pressure and swell potential follow. If it is assumed that the NCL is unique, there are two reasons that the swell potential determined using a stress path from the loading after wetting method with a low soaking stress must always be greater than or equal to the swell potential determined using the soaking-under-load curve:

- Samples cannot swell beyond the NCL into impossible states at zero suction.
- Unless enough softening has occurred such that the path engages the LC yield curve, samples will compress along a swelling line before yielding onto the NCL.

For the same reason, the swell pressure determined using the loading after wetting method ($\bar{p}_{SP,2}$) must always be greater than or equal to the swell pressure determined from the soaking-under-load curve ($\bar{p}_{SP,1}$), since a specimen would need to attain an impossible state beyond the NCL under zero suction to register a greater stress than that upon the NCL when compressed back to the initial void ratio. This is the consensus on the hierarchy of magnitudes of the swell pressure and swell potential determined using the two methods in the literature (Brackley 1973; Justo et al. 1984; Sridharan et al. 1986). Blight (1965) reported a case where the compression curves after soaking and the soaking-under-load curve practically coincided, which also conforms to the aforementioned assumptions (i.e., samples yielded upon completion of inundation as they swelled onto the saturated NCL). In this case, the swell potential functions and the swell pressures determined using the two methods were virtually equal. This phenomenon is most likely to occur in the case of soils that exist in a high degree of saturation range where some form of effective stress law is valid (i.e., the initial degree of saturation exceeds the critical value: $S_0 > S_{crit}$ as discussed by Jennings and Burland (1962)). Note that due to the assumption of a unique NCL, a unique swell pressure value for the loading after wetting method ($\bar{p}_{SP,2}$) is assumed within this framework.

What has not yet been addressed are the swell properties measured during constant volume soaking, followed by unloading. Such a test is given by Path D (1-9-10), which has been added to the previously outlined framework in Fig. 6. The sample is inundated at a constant void ratio and is brought to zero suction along Path 1-9, with a net mean stress equal to the constant volume swell pressure $\bar{p}_{SP,3}$. Hereafter, the sample is unloaded at a constant suction of zero, and elastic volume increase occurs along Path 9-10. If any plastic volume change occurs during soaking under constant net stress, the swell potential estimated from an elastic rebound curve after constant volume soaking should always be less than the swell potential from the other two methods for a highly expansive clay. Gens and Alonso (1992) listed the large plastic volumetric strains during swelling as a defining feature of highly expansive clays. Plastic strains during wetting are accounted for in the framework, which is why the swell potential for *loading after wetting* and *wetting after loading* should both always be greater than the elastic swell potential along a swelling line during *unloading after constant volume soaking*. This is illustrated graphically in Fig. 6 by an evaluation of swell potential at the in-situ net mean stress ($\bar{p}_{in\text{-}situ}$). The swell potentials for

Can. Geotech. J. **62:** 1–25 (2025) | dx.doi.org/10.1139/cgj-2024-0642

Fig. 6. Swell potential and swell pressure for loading after wetting, wetting after loading, and constant volume soaking tests in the BExM framework (after Gens and Alonso 1992).

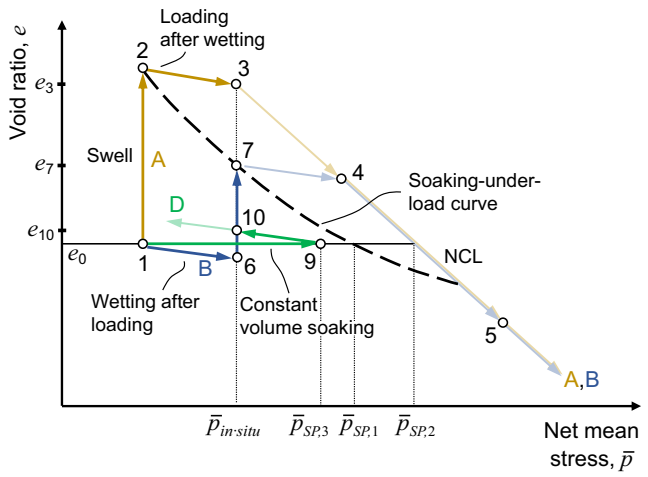

loading after wetting, wetting after loading, and constant volume soaking would be determined by considering the void ratios at Points 3, 7, and 10 respectively, relative to the initial void ratio. It is evident in the framework set out in Fig. 6 that $e_3 \geq e_7 > e_{10}$ for any net stress $\bar{p}_{in\text{-}situ}$ in the swelling range.

The magnitude of the swell pressure measured under constant volume soaking is a more complex matter. Gens and Alonso (1992) explained how the development of swell pressure and the stress path followed under constant volume soaking were highly dependent on initial conditions. The position of the initial state relative to the initial NL line and initial LC curve play a large role in the measured swell pressure, and whether any peak followed by reduction in pressure occurs during soaking. There is no reason for the constant volume stress path to be bound by the soaking-under-load curve. Thus, the peak and equilibrium swell pressures at constant volume may exceed the magnitude determined from a soaking-under-load curve constructed from samples soaked under constant net stress (i.e., $\bar{p}_{SP,3} > \bar{p}_{SP,1}$). Such a result was reported by Sridharan et al. (1986). Although it was not explicitly discussed by the authors, the constant volume swell pressure reported by Monroy et al. (2015) practically coincided with the soaking-under-load curve. It is of course also possible for the constant volume swell pressure to be less than the swell pressure from the soaking-under-load curve (i.e., $\bar{p}_{SP,3} < \bar{p}_{SP,1}$) as reported by Brackley (1973). The dependency on initial state, initial yield loci, and the resulting stress path under constant volume soaking are the reason for the lack of consensus in the literature regarding the magnitudes of the two swell pressures relative to one another. However, no study reports an equilibrium constant volume swell pressure greater than the magnitude measured during a "free swell" followed by consolidation (loading after wetting) test. This is once again due to the fact that a state beyond the NCL cannot be attained when suction has been reduced to zero, and thus it should always be true that $\bar{p}_{SP,2} \geq \bar{p}_{SP,3}$, given a unique NCL.

4. Sampling sites and material classification

Two highly expansive clays were considered in this study. Both soils were alluvially deposited at the sites from which they were sampled, after being transported along watercourses from the nearby residual igneous profiles. The first is a black cotton clay (locally referred to as "turf") weathered from norite and sampled near Steelpoort in the Limpopo Province of South Africa, henceforth referred to as *Black Clay*. The second is an olive/green–grey alluvial bentonite clay, weathered from andesitic and amygdaloidal lavas and sampled near Vredefort in the Free State Province of South Africa, referred to as *Olive Clay*.

The distribution of expansive clays in South Africa, based on records of severe swell-shrink behaviour and associated damage to infrastructure, was given by Williams et al. (1985) and is provided in Fig. 7. The locations of the test sites from which the soils in the current study were sampled have been added to Fig. 7. It is evident that both sites are located in regions where previous records of severe movement of expansive clays exist.

Each of the clays exhibited a fissured or shattered in-situ macrofabric, attributed to the seasonal swelling and shrinkage of the intact clay masses. The X-ray diffraction (XRD) results presented in Table 2 show that despite the different geological origins, the predominant mineral constituent of each clay is smectite – which is the active clay mineral group responsible for the expansiveness of the soils. The Black Clay contains a low quartz content due to the mafic composition of the parent norite rock, whereas the greater silica content in the Olive Clay is likely due to the intermediate felsic/mafic composition of the parent andesitic lava.

Material properties for each of the clays are presented in Table 3 and the respective particle size distributions are presented in Fig. 8. The classification was conducted according to BS 1377-2:1990 and BS 5930:1999. The pycnometer method was used for determination of specific gravity, the fall-cone method for liquid limit, and wet sieving and hydrometer (with sodium hexametaphosphate utilised as the dispersing agent) were employed for determination of the particle size distributions. The in-situ suction was estimated through dewpoint hygrometer and filter paper tests on various samples at the in-situ water content and void ratio at the end of the dry season. These suctions were in the order of several megapascals for both clays.

Despite similar classifications and clay mineralogy, scanning electron microscope (SEM) images showed that a key difference between the two clays, which might contribute to differences in swelling behaviour, is in their microstructural arrangements (i.e., microfabrics). Figure 9*a* shows the continuous matrix of elementary clay particles evident in the Black Clay, such as that of microfabric type *a* described by Gens and Alonso (1992). Figure 9*b* shows the aggregations of elementary clay particles or "packets" evident in the Olive Clay, such as that of microfabric type *b* as described by Gens and Alonso (1992).

Fig. 7. Sampling locations of the two clays, superimposed upon the distribution of expansive clays in South Africa based on records of severe movement (after Williams et al. 1985).

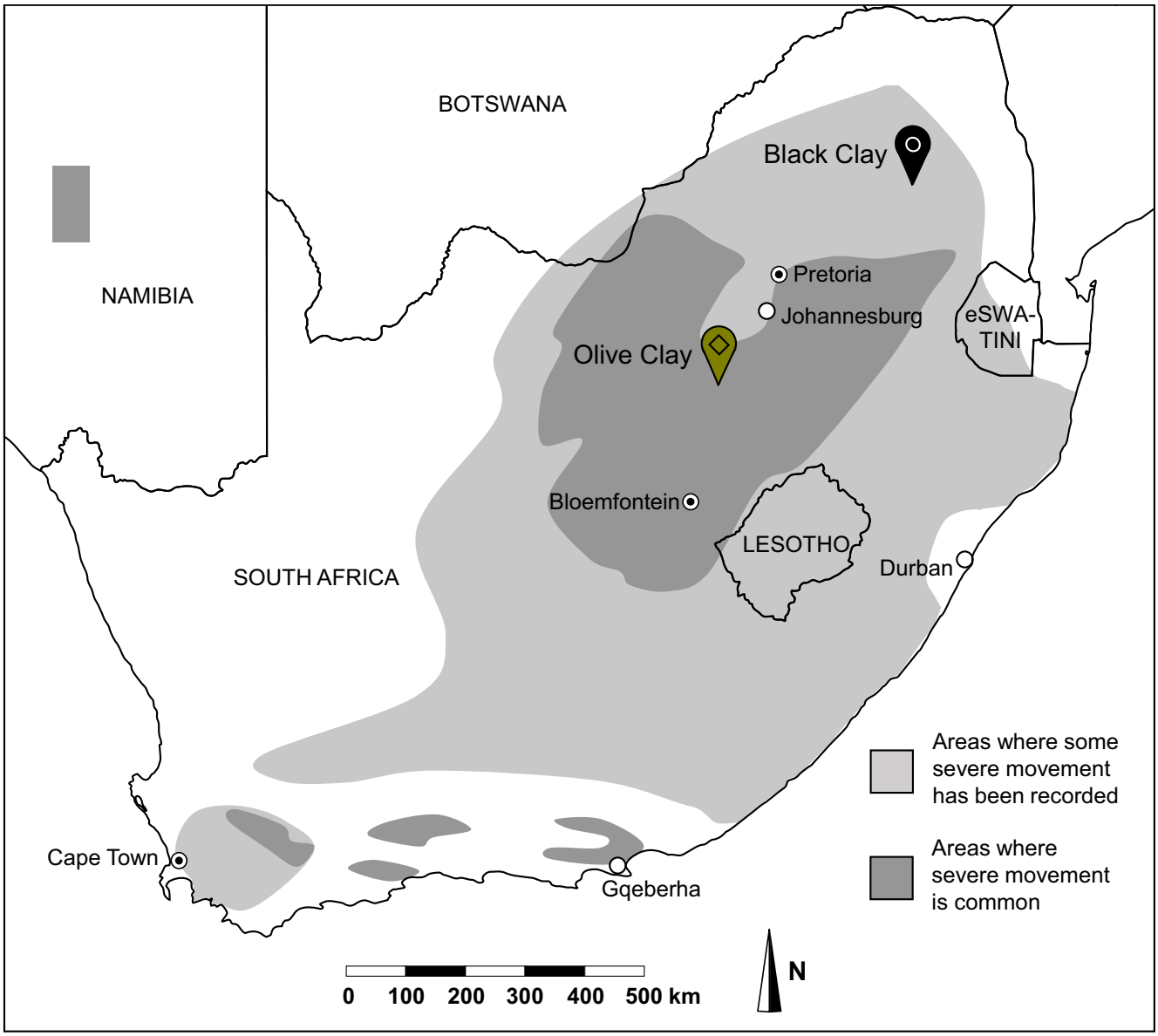

Table 2. Mineralogy from X-ray diffraction (XRD) results.

Mineral	Olive Clay	Black Clay
Quartz (%)	36	7
Orthoclase feldspars (%)	5	11
Anorthoclase feldspars (%)	–	3
Plagioclase feldspars (%)	6	10
Smectite and illite–smectites (%)	52	64
Kaolinite (%)	1	–
Enstatite (%)	–	5

5. Testing programme

As reported in a previous study, oedometer specimens of the Black Clay were prepared by grating intact masses of clay at their natural water content, and then statically compacting the samples to their initial in-situ density (Gaspar et al. 2022). The purpose of this preparation method was to attempt to mimic the fissured macrofabric typical of such clays in situ. Such an approach was not feasible for the Olive Clay as the higher stiffness, brittleness, and presence of silt particles caused difficulties during the grating process. As a result, material preparation methods employed in previous studies on compacted expansive clays (e.g., Monroy et al. 2015; Manca et al. 2016) were employed for the Olive Clay. Bulk samples were air-dried for a minimum period of 30 days to allow for subsequent breaking up of the material with a pestle and mortar until all material passed the 2 mm sieve. Thereafter, the broken-up material was laid flat on a laboratory tray and wetted back to the in-situ water content with a spray bottle, and allowed to equilibrate in a sealed sample bag for 2–7 days prior to testing. The moist clay was statically compacted into oedometer rings, targeting the in-situ dry density presented

Table 3. Properties of the two expansive clays.

Property	Olive Clay	Black Clay
Description of soil in situ (according to profiling guidelines by Jennings et al. 1973*b*)	Slightly moist, olive/green-grey, very stiff, shattered and slickensided, silty clay with scattered calcrete nodules. Alluvium	Moist, black, stiff, fissured and slightly slickensided, silty clay with scattered calcrete nodules. Alluvium
Sampling depth (m)	3.0	0.5–1.5
Specific gravity	2.69	2.65
In-situ dry density, ρ_d (kg/m^3) [a]	1450	1330
In-situ void ratio, e [a]	0.86	0.99
In-situ water content, w (%) [a]	21.5	33.0
In-situ degree of saturation, S (%) [a]	67.5	88.1
Suction at in-situ state, s (MPa) [a]	5–8	2–4
Liquid limit, w_L (%)	109	92
Plasticity index, I_P (%)	82	55
Clay fraction by mass (<2 μm, %)	54	64
Classification (BS 5930:1999)	CE	CE
Activity (Skempton 1953)	1.52	0.86
Potential expansiveness class (Van der Merwe 1975)	Very high	Very high

[a]At the end of the dry season.

Fig. 8. Particle size distributions of the two clays determined according to BS 1377-2:1990.

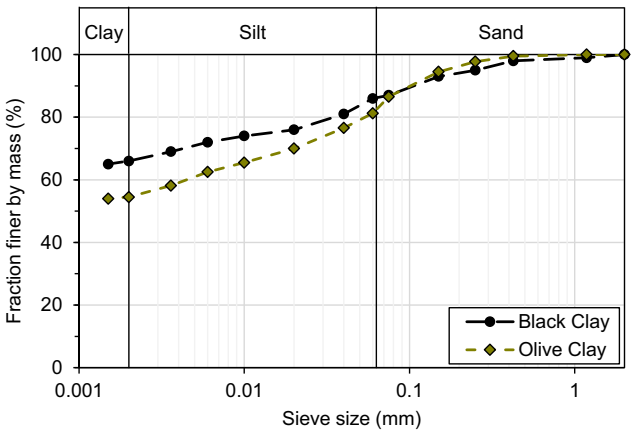

in Table 3. Care was taken to control consistent initial conditions as far as practically possible to limit the experimental variability.

Note that fixed-ring oedometer housings were utilised for all tests in this study. A series of tests on a conventional oedometer apparatus was conducted, utilising various soaking stresses. The samples were placed in the oedometer frame in an unsaturated state, loaded to the desired soaking stress, and the cell was flooded, causing volumetric changes as the sample was brought to a state of zero suction. After equilibrium was achieved, the sample was incrementally loaded, as with a conventional consolidation test, to high stresses (up to 4 MPa). Thereafter, unloading was conducted incrementally. This loading path allows for evaluations of the swell pressure and swell potential to be conducted using both the loading after wetting method (at low soaking stresses) and a soaking-under-load curve from a series of wetting after loading tests. In addition to these swell-under-load tests, constant volume tests were conducted. An automatic oedometer was utilised and the platen position was automatically adjusted to keep the height of the sample constant – as monitored by a linear variable differential transformer (LVDT) fixed to the loading ram – negating any effects of system compressibility. Finally, unsaturated compression tests at constant water content were conducted in a conventional oedometer apparatus. To limit moisture loss from the specimen, single layers of Teflon were provided at the top and bottom of the sample, and single layers of clingfilm were fixed to the top and bottom of the sample ring using elastic bands, taking care to avoid any folds that would impose bedding errors. The specimen was placed in the standard oedometer housing, which was carefully sealed using clingfilm and not flooded with water.

For each increment in each of the tests, deformation readings throughout compression/swelling were logged using an LVDT and the given increment was only ended at the end of primary compression or swell (characterised by an abrupt change in slope on the semi-logarithmic plot of volume change versus time). The exception was the unsaturated constant water content test, where the benefit of limiting moisture loss over time was deemed to exceed that of allowing the completion of primary compression. For this reason, increments were limited to 24 h. This was deemed sufficient as the majority of deformation took place within the first hour of loading.

Reconstituted samples were prepared by thoroughly remoulding the air-dried and crushed clay at a water content between 1.0 and 1.5 times the liquid limit, as suggested by Burland (1990). Table 4 lists the initial conditions for each of the tests conducted on the Olive Clay.

A similar series of swell-under-load tests was reported by Gaspar et al. (2022) for the Black Clay. The soaking phases of two of these tests, as well as the entire reconstituted test, were used in this study. These tests were supplemented with an additional six swell-under-load tests, which were

Fig. 9. Scanning electron microscope (SEM) photographs showing the microstructural arrangements of (*a*) Black Clay and (*b*) Olive Clay.

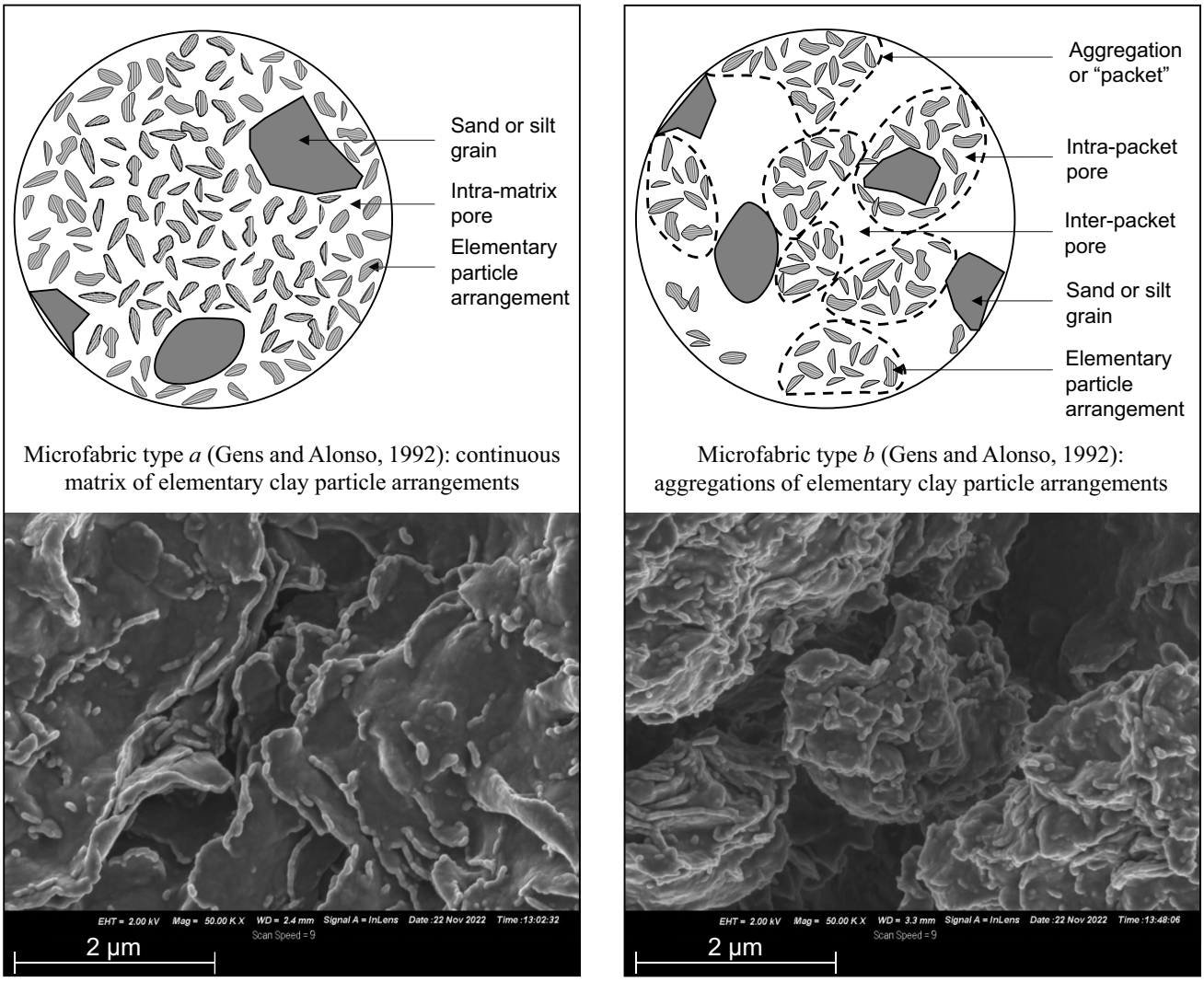

a) Black Clay: BExM microfabric type *a*

b) Olive Clay: BExM microfabric type *b*

Table 4. Initial conditions for tests on compacted Olive Clay.

Soaking stress (or test name)	Initial void ratio, e_0	Initial water content, w_0 (%)	Initial degree of saturation, S_0 (%)
1.1 kPa	0.864	21.4	66.7
12.5 kPa	0.849	21.9	69.5
50 kPa	0.831	21.4	69.5
100 kPa	0.850	21.7	68.7
300 kPa	0.843	22.7	72.5
400 kPa	0.855	20.0	63.0
600 kPa	0.875	21.9	67.4
1200 kPa	0.856	20.0	62.9
Unsaturated (constant *w*)	0.847	21.9	69.7
Constant volume soaking	0.830	20.3	65.9
Reconstituted[a]	3.924	$147.0 \approx 1.3w_L$	100

[a]Not compacted.

consolidated to high stresses, as well as a constant volume soaking test and an unsaturated constant water content test (all on grated and compacted material). Table 5 lists the initial conditions for each of the Black Clay tests.

6. Results

6.1. Intrinsic properties

Burland (1990) proposed that clay samples reconstituted at water contents of between 1.0 and 1.5 times the liquid limit may be used to determine the intrinsic compression properties of the clay (i.e., properties that are independent of soil state and structure). The NCL that is measured for such a sample is thus referred to as the intrinsic compression line (ICL). The ICL can be defined in terms of the intrinsic void ratios e^*_{100} and e^*_{1000}, which correspond to void ratios measured at effective stresses of 100 and 1000 kPa, respectively, as well as the intrinsic compression index, $C^*_c = e^*_{100} - e^*_{1000}$. In this study, the intrinsic expansion index (C^*_e) has also been defined by taking the slope of a logarithmic best-fit line through the full unloading range. The modified free swell index proposed by Sivapullaiah et al. (1987) was used as an indicator of the intrinsic expansiveness of the clay due to inundation with water. This involves passing oven-dried and crushed clay through a 0.425 mm sieve and slowly adding 10 g of the material to distilled water in a graduated cylinder. The modified free swell index is given by $(V - V_s)/V_s$, where V is the equilibrium volume of clay after settling and swelling, and V_s is the volume of solids (determined from the specific gravity and mass of solids). Intrinsic properties for both clays are reported in Table 6. The Black Clay exhibited a greater intrinsic expansiveness due to absorption of water, whereas the Olive Clay exhibited greater intrinsic compressibility and expansiveness due to changes in effective stress.

6.2. Swell and collapse phases

Figure 10 shows the volumetric strain over time for the compacted samples during soaking phases under constant vertical stress, where expansion is taken to be negative. The Olive Clay was shown to be more expansive than the Black Clay over the full range of soaking stresses.

Figure 11 illustrates the degree of swell, which is the current volumetric strain (ε_v) normalised by the maximum swelling strain ($\varepsilon_{v,min}$, due to geotechnical sign convention where expansion is negative), as a function of time for the two sets of samples. These results indicate that for the Olive Clay samples, the time required to achieve a particular degree of swell reduced with an increase in soaking stress. Conversely, for the Black Clay samples, the time required to achieve a particular degree of swell increased with an increase in soaking stress. The reasons for these conflicting trends may be hypothesised by considering the different macrofabrics of the two clays due to sample preparation. When an expansive clay is inundated with water, there are two potential mechanisms which influence ingress. For a continuously fissured sample, initial ingress occurs relatively quickly along the fissures, allowing for a rapid initial swell process and closure of fissures. Thereafter, further infiltration into the macrostructure and microstructure becomes a diffusive process which is governed by the square of the drainage path length. By examining the swell behaviour with time of the two clays, the influences of these two mechanisms can be seen.

Due to the preparation method, the Black Clay had an initial macrofabric that incorporated continuous “fissuring”. As a result, initial swell was facilitated relatively quickly. This can clearly be seen by comparing samples of both clay types soaked at a vertical stress of 1.1 kPa. The time taken to achieve a degree of swell of 0.2, for example, for the Black Clay was approximately 2 orders of magnitude less than that of the Olive Clay. As soaking stresses were increased however, some closure of the fissures would have occurred in the Black Clay prior to inundation, thereby reducing the influence of this initial infiltration phase. In such cases, the swell process would have been more dependent on diffusion from the start of inundation. Additionally, the rate of infiltration into the intact masses from the fissures is reduced under greater confining stress. Therefore, for the series of Black Clay tests as a whole, the degree of swell over time as a function of soaking stress was governed by the suppression of infiltration with increasing stress, rather than the increasing drainage path length with decreasing stress.

For the Olive Clay, which was crushed rather than grated prior to compaction, no such continuous fissures were present. The swell process would thus have been dominated by diffusion from the start of inundation for all tests. Given that diffusion is governed by the drainage path length squared, the time to equilibrium swell was largest for the samples that were subjected to the largest swelling strains (i.e., those soaked under low soaking stresses). Equilibration time reduced as swell magnitude reduced with an increase in soaking stress. Significantly larger swelling strains were experienced by the Olive Clay, which further supports the observation of equilibration times that were orders of magnitude greater at low stresses. In contrast to the Black Clay, the degree of swell over time as a function of soaking stress for the Olive Clay was governed by the increasing drainage path length with decreasing stress rather than the suppression of infiltration with increasing stress.

Another key difference in the behaviour of the two samples was evident in the initial volumetric changes experienced during inundation. For all samples of the Black Clay soaked under stresses less than the swell pressure, only expansion occurred with the introduction of water. Conversely, for the Olive Clay tests (with the exception of the sample soaked under 1.1 kPa), all samples inundated at stresses less than the swell pressure exhibited initial collapse, followed by swell. This difference in behaviour can be attributed to differences in microfabric. Gens and Alonso (1992) highlighted that the aggregated microfabric of the Olive Clay is a fabric type which has the potential to both collapse and swell upon wetting. A closer inspection of the initial collapse strains exhibited in the Olive Clay tests is presented in Fig. 12. This figure shows that initial reduction in volume occurred significantly quicker than the subsequent swelling strains, indicating the occurrence of two separate mechanisms. Initially, a reduction in suction between clay aggregations causes

Table 5. Initial conditions for tests on compacted Black Clay.

Soaking stress (or test name)	Initial void ratio, e_0	Initial water content, w_0 (%)	Initial degree of saturation, S_0 (%)
1.1 kPa	1.034	33.7	86.4
12.5 kPa	0.999	34.8	92.2
50 kPa	1.006	34.8	91.6
100 kPa	0.995	33.0	87.9
200 kPa*	0.973	34.7	94.4
300 kPa	0.992	34.3	91.7
400 kPa*	1.027	34.7	89.4
800 kPa	0.996	33.8	89.8
Unsaturated (constant w)	0.996	32.6	86.7
Constant volume soaking	0.996	33.8	89.8
Reconstituted*,[a]	2.481	$98.5 \approx 1.1 w_L$	105[b]

*Test reported by Gaspar et al. (2022).
[a]Not compacted.
[b]Can be attributed to slight error in initial void ratio, which can be problematic for a slurry.

Table 6. Intrinsic properties of the Olive Clay and Black Clay.

Property	Olive Clay	Black Clay
Void ratio at the liquid limit, e_L	2.942	2.438
Intrinsic void ratio at 100 kPa, e^*_{100}	2.141	1.388
Intrinsic void ratio at 1 MPa, e^*_{1000}	0.807	0.849
Intrinsic compression index, C^*_c	1.334	0.539
Intrinsic expansion index, C^*_e	0.237	0.110
Modified free swell index (Sivapullaiah et al. 1987)	5.37	6.16

Fig. 10. Volume change over time under various soaking stresses for both clays.

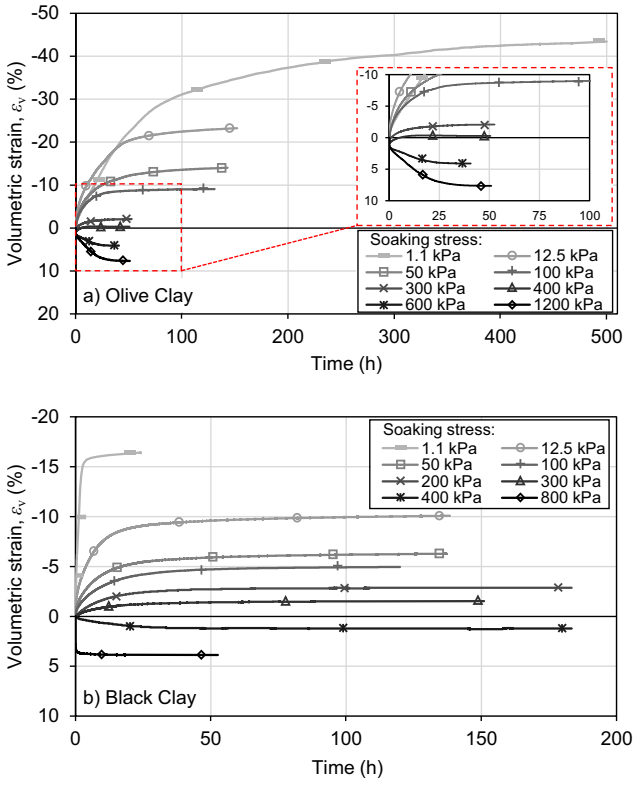

Fig. 11. Degree of swell over time at soaking stresses under which expansion occurred.

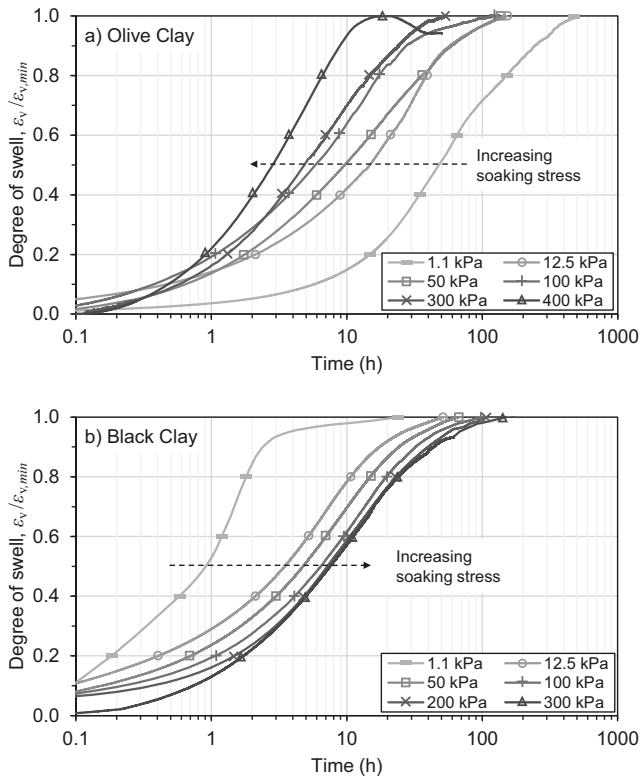

the observed macrostructural collapse. Thereafter, the slower process of clay hydration ensues, resulting in microscopic and eventually macroscopic swell.

6.3. Soaking-under-load curves

The difference in swell properties of each clay is illustrated through the soaking-under-load curves presented as functions of volumetric strain and void ratio in Figs. 13*a* and 13*b*, respectively. For both clays, the soaking-under-load curve can be represented as a logarithmic relationship (a straight line in semi-log space) with coefficients of determination exceeding

Fig. 12. Initial collapse of the Olive Clay samples for which expansion occurred.

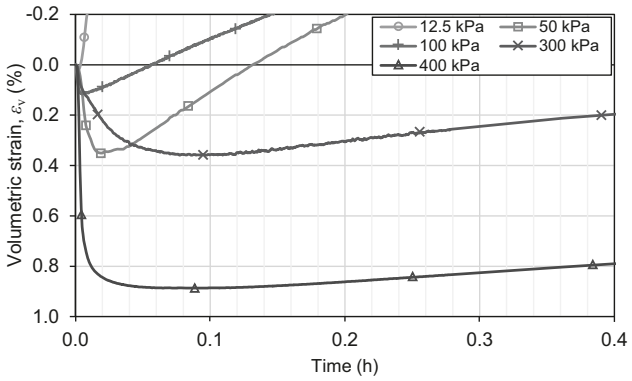

Fig. 13. Soaking-under-load curves for the Olive and Black Clays: (*a*) volumetric strain versus net vertical stress at equilibrium after soaking; (*b*) void ratio versus net vertical stress at equilibrium after soaking.

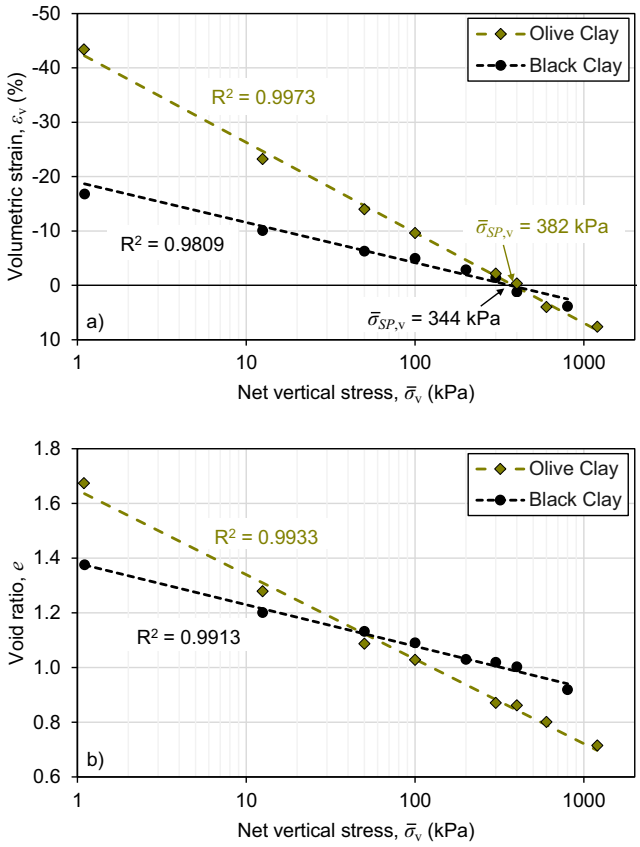

98% in terms of volumetric strain and exceeding 99% in terms of void ratio. Note that the stress state variable used when interpreting the swell tests (and any phases where the clay was in an unsaturated state) is net vertical stress ($\bar{\sigma}_v = \sigma_v - u_a$), where σ_v is the applied total vertical stress and the pore air pressure (u_a) is assumed to be zero. Vertical swell pressures ($\bar{\sigma}_{SP,v}$) of 382 and 344 kPa were recorded using the soaking-under-load curve method for the Olive and Black Clays, respectively.

Previous authors have reported differently shaped relationships for the soaking-under-load curves of various high plasticity expansive clays, all predominantly consisting of montmorillonite. Brackley (1973) also reported a logarithmic relationship for a black weathered residual norite clay (w_L = 89%, I_P = 57%) from Onderstepoort, South Africa. The best-fit soaking-under-load curve for London Clay from results by Monroy et al. (2015) (w_L = 83%, I_P = 54%) had the same shape. Al Haj and Standing (2015) reported a power function for the soaking-under-load curve of a basaltic alluvial black clay from Khartoum, Sudan (w_L = 60%, I_P = 30%). Fourie (1991) illustrated that the relationship was approximately linear for a sedimentary black clay from Queensland, Australia (w_L = 89%, I_P = 63%). Justo et al. (1984) reported a relationship where swell potential was a third-order polynomial function of the logarithm of applied stress for a sedimentary expansive clay sampled at El Arahal, Andalucía (w_L = 75%, I_P = 44%).

Whilst recognising these previously reported trends, it should be noted that the stress range over which the soaking-under-load curve is established will affect this relationship. While more complex functions may be necessary to define the relationship over a wide stress range or at specific stress levels (as may be desirable in specialised cases), simpler relationships may be adequate over typical engineering stress ranges. Despite significant differences in the respective geologic origins, it holds true for each of the aforementioned studies that a logarithmic soaking-under-load curve fitted through data from the entire range of soaking stresses would yield a coefficient of determination exceeding 95%. Excluding the study by Al Haj and Standing (2015), this can be increased to 98% if only tests soaked under a stress within two log-scales of the swell pressure are considered. Recognising this feature, practitioners may be able to conduct fewer tests during field characterisations.

6.4. Loading after wetting

The compression paths after soaking are given in Fig. 14. It is evident that significant variations in swell pressure were recorded for both clays depending on the seating stress under which the sample was soaked. For the Olive Clay, swell pressures ranging between 423 and 578 kPa were recorded using this method. Swell pressures recorded for samples soaked at low stresses (1.1, 12.5, 50 kPa) were similar. As the soaking stress increased, the recorded swell pressure reduced and approached the magnitude determined from the soaking-under-load curve.

For the Black Clay, a similar trend may have been evident, but was masked by the non-uniqueness of the NCL. The maximum swell pressure was that of the sample soaked under 100 kPa. Swell pressures recorded using this method ranged between 364 and 437 kPa. However, it is worth noting that the initial void ratio of the 1.1 kPa test was marginally greater than the target in-situ void ratio. As a result, the swell pressure recorded at the actual initial void ratio (~1.03) was a reduced value of 364 kPa, whereas the swell pressure that would have been recorded if the target initial void ratio was achieved would likely have been greater. As an example, the

Fig. 14. Loading after wetting paths.

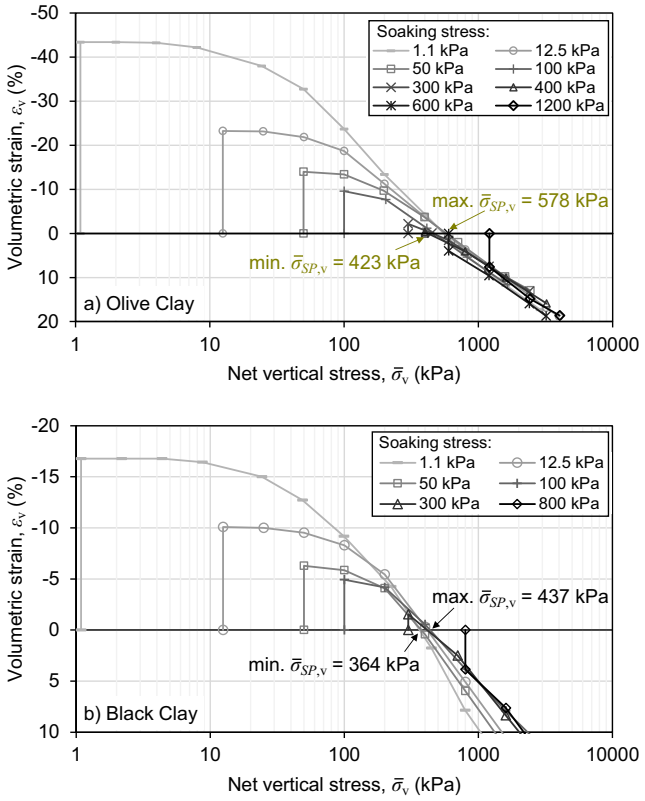

Fig. 15. One-dimensional consolidation test results.

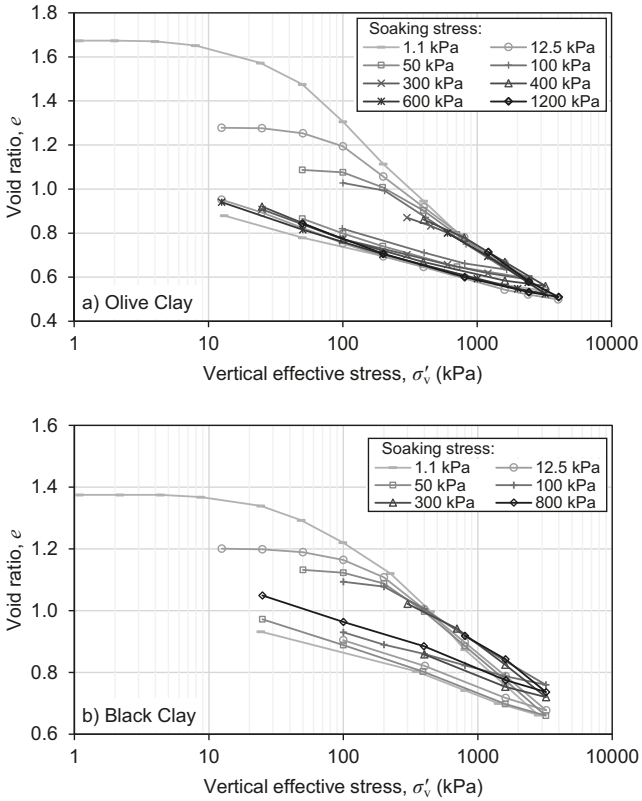

stress corresponding with the in-situ void ratio (0.99) upon the stress path for this test was 463 kPa.

The non-uniqueness of the NCL for compacted Black Clay was attributed to destructuring invoked during swelling and the release of strain energy, which is discussed in the subsequent section.

6.5. Normal consolidation lines

Figure 15 shows the compression and unloading paths for each of the tests in terms of void ratio and effective stress, so that the NCLs for the compacted samples could be established. These results are plotted in terms of traditional vertical effective stress ($\sigma'_v = \sigma_v - u_w$), where the pore water pressure (u_w) is approximately zero at the end of consolidation, so that they may be interpreted within a saturated soil mechanics framework. As a result, the soaking phases have not been included in Fig. 15, since effective stress is not applicable at the initial state.

For the Olive Clay, loading paths converged onto a unique NCL at stresses greater than approximately 800 kPa as illustrated in Fig. 15*a*, and the compression index values (taken as the slope of a best-fit line over the entire post-yielding range) ranged between 0.37 and 0.40. For the compacted Black Clay, there were seemingly two sets of NCLs. The samples soaked at 1.1, 12.5, and 50 kPa exhibited similar compression indices (0.37–0.39), and the samples soaked under 100, 300, and 800 kPa also exhibited similar C_c values (0.29–0.33). Leroueil and Vaughan (1990) proposed that strain energy stored within the structure of soils and rocks is released during the destruction of structural bonds, which may occur during swell. When subjected to large swelling strains, the structure in the Black Clay was unable to retain some of the stored energy. The suggested reason for two sets of NCLs is thus the release of the stored strain energy due to destructuring imposed during the swelling process under low soaking stresses. Maximum swelling strains of approximately 7% and greater were imposed during soaking for these samples, and destructuring caused the compression indices to increase and tend toward the intrinsic compression index (C_c^*). However, at greater soaking stresses, where swelling strains were suppressed to a greater degree, structure was likely preserved. This allowed higher void ratios to be attained at the same effective stress for these samples in comparison to those that had been destructured.

The dependency of the Black Clay compression index on the strain imposed during soaking is illustrated in Fig. 16*b*, where two groupings of C_c values can be observed (at absolute soaking strains less than and greater than 5%). Interestingly for the Olive Clay, the compression index is shown to be independent of the strain imposed during soaking in Fig. 16*a*, despite significantly greater strains being achieved during swelling at low stresses (swelling strains in excess of 43% and 23% were observed in the 1.1 and 12.5 kPa tests, respectively). In addition, the compression indices for the compacted samples were substantially lower than the intrinsic compression index from the reconstituted test (by factors of between 3.3 and 3.8), indicating the presence of some structure in each of the tests.

It seems that significantly greater swelling strains would be required to destructure the crushed and compacted Olive

Can. Geotech. J. **62:** 1–25 (2025) | dx.doi.org/10.1139/cgj-2024-0642

Fig. 16. Compression and expansion indices as functions of soaking strain.

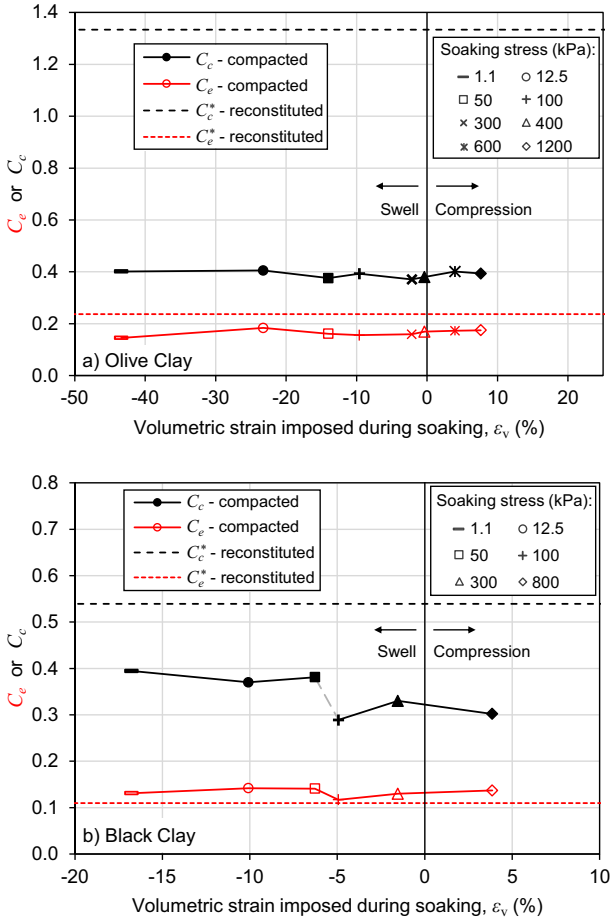

Clay with the aggregated microfabric (type *b*) than for the grated and compacted Black Clay containing a continuous matrix of elementary clay units in its microstructural arrangement (type *a*). This suggests that the structure within the Olive Clay was more robust, with an ability to retain stored strain energy despite being subjected to larger swelling strains.

Neither of the sets of tests showed any influence of soaking stress upon the expansion indices (C_e), which remained fairly constant. For the Olive Clay, the expansion indices for compacted samples were 1.3–1.6 times lower (i.e., stiffer) than the intrinsic expansion index (C_e^*), which once more illustrates the influence of stored strain energy due to the preservation of soil structure, even after being subjected to compressive stresses of up to 4 MPa. For the Black Clay, compacted expansion indices were similar in magnitude to the intrinsic expansion index (1.0–1.3 times greater, i.e., softer).

6.6. Yield stresses

Graphical constructions using the methodology recommended by Casagrande (1936) were used to determine vertical yield stresses ($\bar{\sigma}_{v,y}$) for each of the tests that were soaked at low enough stresses such that the sample was overconsolidated after soaking. Trends of increasing yield stress with

Fig. 17. Relationship between soaking stress, yield stress, and swell: (*a*) swell governed by proximity to LC yield curve in BExM (after Gens and Alonso 1992); (*b* and *c*) swell magnitude versus proximity to LC yield curve for the Olive and Black Clays.

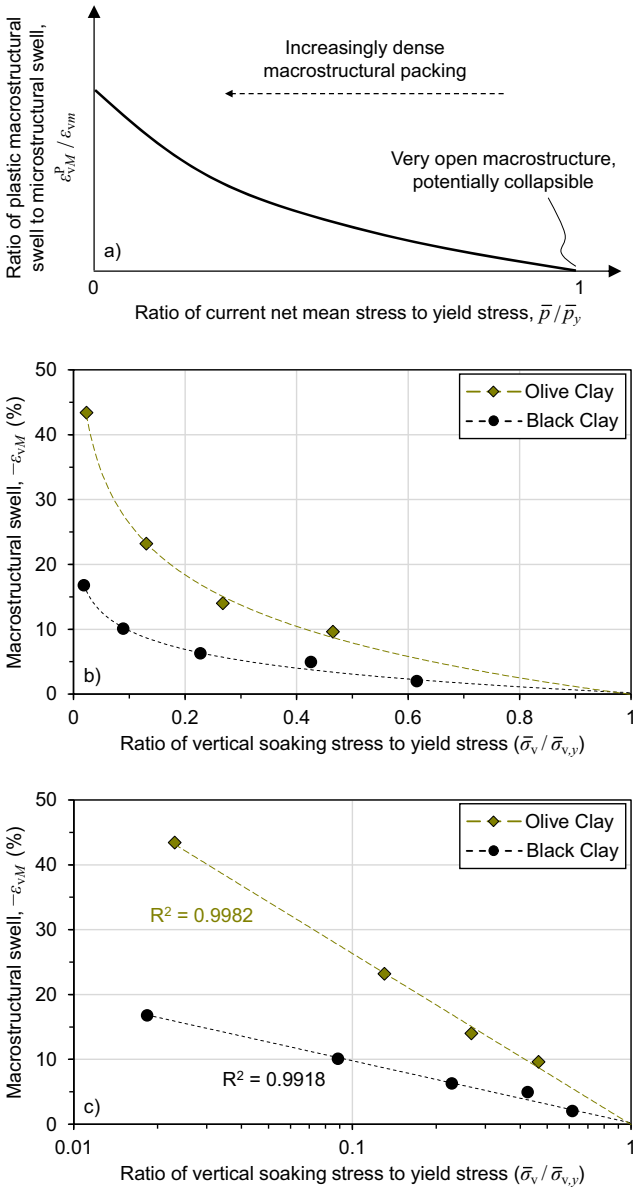

increasing soaking stress were evident for both clays. The decrease in yield stress at lower soaking stresses can be attributed to (a) the higher void ratio attained after swell, and (b) the greater amount of swell-induced softening at lower soaking stresses, as a result of the greater microstructural volume change.

Figures 17*b* and 17*c* show the macrostructural volume increase ($-\varepsilon_{vM}$) versus the ratio of the soaking stress to the yield stress (i.e., induced swell as a function of the proximity of the wetting path to a yield surface). Logarithmic best-fit relationships with coefficients of determination exceeding 99% were determined for both clays. The shape of the function aligns with the conceptual relationship that highlights

Fig. 18. Developed swell pressure versus time during constant volume soaking for both clays.

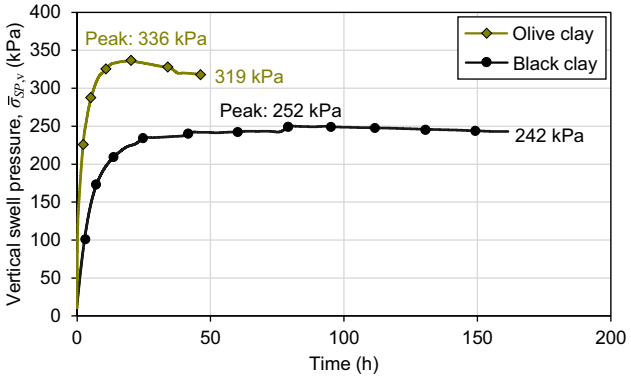

Fig. 19. Constant volume soaking followed by unloading paths, relative to one-dimensional consolidation and unloading paths.

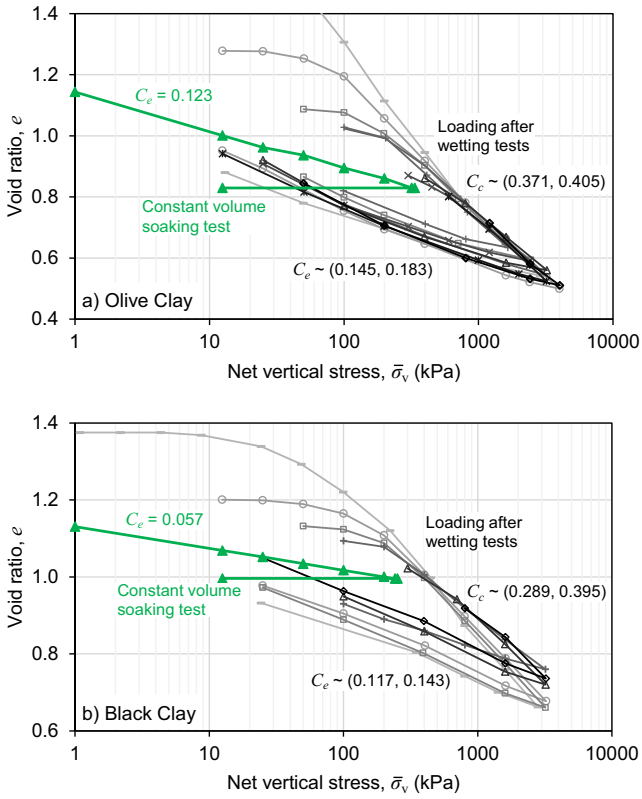

how macrostructural swell is governed by proximity of the wetting path to the LC yield curve in the BExM framework (Gens and Alonso 1992), which is shown in Fig. 17*a*. Gaspar et al. (2022) highlighted that this relationship typically considers microscopic volume change, which is difficult to measure and requires sophisticated equipment. However, the study showed that a similar relationship could be obtained when considering only macrostructural deformation. This implied that useful constitutive criteria governing hardening plasticity can potentially be deduced using conventional equipment. The results reported in the current study provide further experimental evidence of these trends for clays with both types of microstructural arrangement.

6.7. Constant volume soaking

The development of vertical swell pressure over time under constant volume inundation is given for both clays in Fig. 18. Both samples exhibited a peak swell pressure, followed by a slight reduction over time until equilibrium conditions were achieved. As discussed previously, the hypothesised mechanism for the observed trends regarding equilibration time during constant stress swelling (Fig. 11) was related to the relative contributions of diffusive processes and seepage through macrofissures in governing the swell of the two clays. In the constant volume tests, the sample height (and thus the drainage path length) remained constant. For this reason, the contribution of the diffusive swelling process to time to equilibrium was suppressed for the Olive Clay (since the large swelling strains that had increased the drainage path length in the soaking-under-load tests were no longer generated). The slower development of constant volume swell pressure in the Black Clay can be attributed to the grated macrofabric. Initial swell needed to occur internally to close the fissures, before swell pressures were externally recorded on a macroscopic scale. Due to the lesser degree of macrostructural fissuring in the Olive Clay samples, the tendency to swell was more rapidly transferred into developed swell pressure. The peak vertical swell pressures measured under *constant volume soaking* were less than those measured using the *loading after wetting* and *wetting after loading* methods for both clays.

After soaking, the samples were unloaded incrementally with each increment continuing until the completion of primary swell, allowing for the estimation of swell potential as per the method described by Sullivan and McClelland (1969). The stress paths followed during soaking and unloading are illustrated along with all other oedometer test results in Fig. 19. The NCLs were not engaged during constant volume soaking for either clay. Additionally, slopes of the unloading lines (i.e., expansion indices, C_e) were lower than those measured in all other oedometer tests for both clays.

6.8. Constant water content tests

Constant water content tests were conducted by sealing the sample and oedometer housing such that minimal loss of moisture would occur throughout loading. The entire sealed housings, as well as the samples, were weighed before and after testing to determine whether moisture loss had occurred. Using the change in mass of the sealed housing, water content reductions of approximately 1% for both the Black and Olive Clay were recorded (and deemed acceptable). However, the sample masses decreased such that a water content reduction of approximately 3% and 5% were recorded for the Olive and Black Clays, respectively. Some condensation was noted on the inside of the housings. It is likely that the loss of moisture of the samples was enforced by squeeze-out of water as the samples approached full saturation due to reduction in volume after yielding.

Can. Geotech. J. **62:** 1–25 (2025) | dx.doi.org/10.1139/cgj-2024-0642

Although suction control was not imposed, it is likely that the suction would have remained approximately constant prior to yielding. Monroy et al. (2015) found that expansive clay samples that were loaded or unloaded under constant suction conditions exhibited negligible changes in gravimetric water content, despite the volume changes invoked due to changes in net stress. The authors thus proposed that the relationship between water content and suction was unique (i.e., not dependent on changes in void ratio), due to the fact that suction is dominated by adsorption effects beyond a certain threshold (Baker and Frydman 2009). This value was suggested to be 400 kPa by Baker and Frydman (2009) for the London Clay tested by Monroy (2005), and between 100 and 400 kPa for various other soils. Monroy et al. (2015) found that the unique suction–water content relationship held true for suctions beyond 115 kPa. As shown in Table 3, the suction values for the initial states of the Olive and Black Clays would be an order of magnitude greater than this threshold. Further evidence of the unique suction–water content relationship was presented in soil–water retention curves for the Olive Clay tested in this study by Murison et al. (2023). Samples were prepared over a range of initial void ratios, and full primary drying and wetting curves were measured. Despite observable differences in the suction–degree of saturation and suction–void ratio relationships due to density, there were insignificant differences due to density in the suction–water content relationships for both drying and wetting.

The results are given along with parallel tests where the cell was inundated with water, as suggested for the double oedometer test (Jennings and Knight 1957), in Fig. 20. For the constant water content test, where suction (s) greater than zero was present, the slope for the unloading path was termed $C_e(s)$. For the test where the sample was allowed to achieve a state of zero suction prior to loading, the slope of the unloading path was termed $C_e(0)$. The slopes of the elastic regions (non-virgin states) for loading and unloading were significantly flatter for the constant water content test than for the test soaked prior to loading (i.e., $C_e(0) > C_e(s)$), for both clays. This highlights an acknowledged limitation in the simplifying assumption in the original Barcelona Basic Model (Alonso et al. 1990) that the slope of loading paths in non-virgin states (κ) is not a function of suction (i.e., $\kappa(s) = \kappa(0)$).

The unsaturated samples for both clays exhibited sharp yielding, followed by a loading path approximately parallel to the "saturated" NCL. The slopes of the post-yielding loading paths (virgin states) for the natural water content and inundated tests have been termed $C_c(s)$ and $C_c(0)$, respectively. The yield point was at approximately 1600 kPa for the Olive Clay and 800 kPa for the Black Clay. If it is assumed that no change in water content occurred prior to yielding, the Olive Clay and Black Clay samples yielded at degrees of saturation of 82.3% and 92.5%, respectively. If it is then assumed that all loss of moisture had occurred by the end of the final loading increment, degrees of saturation of approximately 100% had been achieved for both tests. This large increase in degree of saturation may have caused a significant post-yielding reduction in suction, which is the proposed reason for similar magnitudes between $C_c(0)$ and $C_c(s)$ for both clays. If constant suction conditions had been enforced post-yielding, a greater reduction in magnitude of C_c due to suction would be expected as suggested by Alonso et al. (1990) (where the value of $\lambda(s)$ reduces with increasing suction).

Fig. 20. Double oedometer test results.

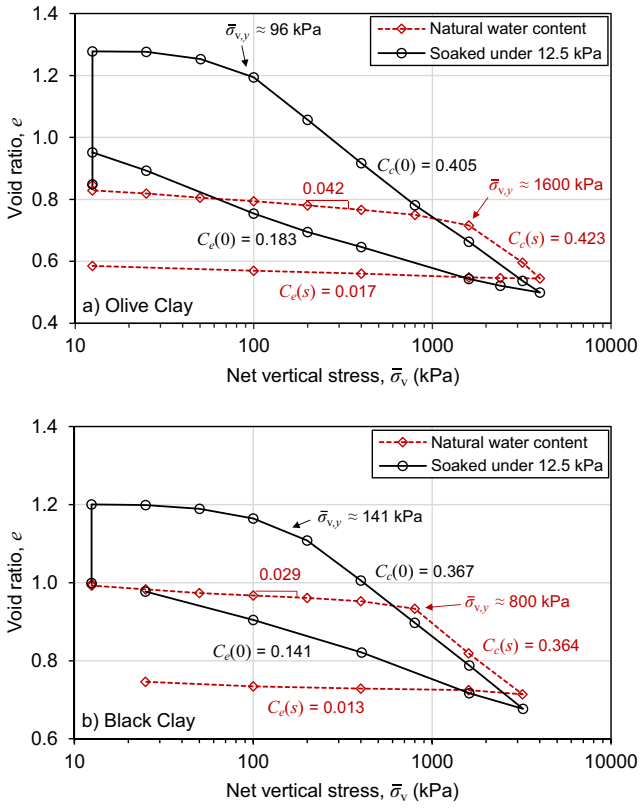

Jennings and Kerrich (1962) noted that the theory of coincidence of the saturated and unsaturated curves, as discussed earlier and illustrated in Fig. 1, is only applicable when the traditional principle of effective stress holds for partially saturated soils. Jennings and Burland (1962) had shown experimentally that the principle is only valid over a limited range of partial saturation. The degree of saturation (S) value below which the traditional principle of effective stress would no longer hold for a particular soil was referred to as the critical degree of saturation (S_{crit}). It was suggested that for degree of saturation values lower than S_{crit}, the soil no longer obeys the principle that a reduction in "effective stress" results in volume expansion. Burland (1962) suggested that this can be seen experimentally through a "cross-over" for the natural water content and soaked compression paths in the double oedometer test, due to the inequivalence of changes in suction and confining stress. Therefore, for samples prepared at an initial degree of saturation (S_0) less than the critical saturation, any correction of the natural water content curve to facilitate coincidence of the curves would result in a gross overprediction of swell potential. Jennings and Kerrich (1962) noted that degrees of saturation less than S_{crit} are common for very dry soils and at depths near the ground surface. The cross-over is evident in the double oedometer test results for both clays in Fig. 20. It should also not be surprising that the traditional law of effective stress does not ap-

Table 7. Swell pressure determined from different methods.

Test method		Vertical swell pressure, $\bar{\sigma}_{SP,v}$ (kPa)	
		Olive Clay	Black Clay
Soaking-under-load curve (from a series of wetting after loading tests)		382	344
Constant volume soaking		336	252
Loading after wetting tests	Soaking stress:		
	1.1 kPa	554	364 (463*)
	12.5 kPa	567	417
	50 kPa	578	375
	100 kPa	467	437
	300 kPa	458	414
	400 kPa	423	–

*If the target void ratio instead of initial void ratio is used.

ply within the tested range of initial conditions. If the classical law of effective stress for saturated soils (i.e., $\sigma' = \sigma - u_w$: Terzaghi 1936) applies, soil behaviour in response to changes in porewater pressure and changes in external (total) stress are equivalent. If these changes were equivalent, the samples would have pre-consolidation pressures (i.e., yield stresses) of at least equal magnitude to the initial suction. The result of these assumptions is that if a sample was wetted to a state of zero suction and loaded until it was compressed back to its initial void ratio, the imposed total stress (which is the swell pressure) would be equal to the initial suction. As indicated in Table 3, the initial suctions were in the order of 5–8 MPa for the Olive Clay samples and 2–4 MPa for the Black Clay samples, but the swell pressures measured for the samples were in the order of 0.34–0.58 MPa and 0.25–0.44 MPa for the respective clays. The fact that the swell pressure is at least an order of magnitude lower than the initial suction is substantial evidence that a traditional effective stress law cannot apply to either of the clays, given their in-situ state, and highlights the value in considering net stress and suction as separate stress state variables.

6.9. Summary of results

6.9.1. Similarities between the two clays

The swell pressure determined for each of the methods for both clays is given in Table 7. For both clays, the greatest swell potential and swell pressure were determined using a *loading after wetting* test. The soaking-under-load curves constructed from series of *wetting after loading* tests gave lower values for swell pressure and swell potential. Finally, the *constant volume soaking followed by unloading* tests yielded the lowest swell pressures and swell potential functions over the entire stress range for both clays.

For both clays, the hierarchy of swell pressure and swell potential magnitudes determined from the different methods were in agreement with the BExM framework (Gens and Alonso 1992) discussed in Section 3. Within the framework, one unique swell pressure value for the loading after wetting method ($\bar{p}_{SP,2}$) is assumed due to the unique NCL. This was not observed for either of the clays reported in this study. In the case of the Olive Clay, the reason for a non-unique loading after wetting swell pressure is that compression paths only converged onto the unique NCL at stresses greater than any recorded swell pressure. For the Black Clay, an additional variation of these swell pressures was observed since the NCL was non-unique due to differing effects of soil structure between tests.

An interesting feature in Fig. 5 is the coincidence of the constant suction loading curve, the soaking-under-load curve, and the saturated NCL at a common point, indicated by Point "O". This common point is intuitive if one considers a sample loaded at constant suction until the state of the soil (void ratio and net stress) coincides with the saturated NCL. When this sample is wetted to zero suction under a constant net stress on the NCL, no volume change should occur. If the slope of the constant suction loading path was zero (i.e., no volume change occurs when the sample is loaded under the constant given suction), then the swell pressures $\bar{p}_{SP,1}$ and $\bar{p}_{SP,2}$ would be equal. It thus follows that the flatter the slope of the loading path at constant suction prior to yielding, the closer the swell pressures determined from the wetting after loading and loading after wetting methods should be. This is evident given the results for the two clays. As illustrated in Fig. 20, the Black Clay exhibited a greater pre-yielding stiffness at constant water content for its in-situ state than that of the Olive Clay (indicated by a slope of 0.029 versus 0.042). The maximum variation between the vertical swell pressures using a loading after wetting test and the soaking-under-load curve for the Black Clay was 27%, which is significantly less than the variation of 51% recorded for the Olive Clay. Of course, another situation in which swell pressures $\bar{p}_{SP,1}$ and $\bar{p}_{SP,2}$ would be nearly equal, regardless of the slope of the natural water content loading path, is when the NCL and soaking-under-load curve coincide over the entire stress range (as reported in the study by Blight 1965). This case is not applicable to the results of the current study.

Figure 21 summarises the results for each of the methods for both clays by depicting the stress paths in the void ratio versus net stress plane, in a similar fashion to that derived from the BExM framework in Figs. 5 and 6. Figure 21*a* illustrates the intersection of the constant water content loading path, the NCL, and soaking-under-load curve at a single com-

Fig. 21. Test results for swell properties of the two clays using all three methods, agreeing with the BExM framework.

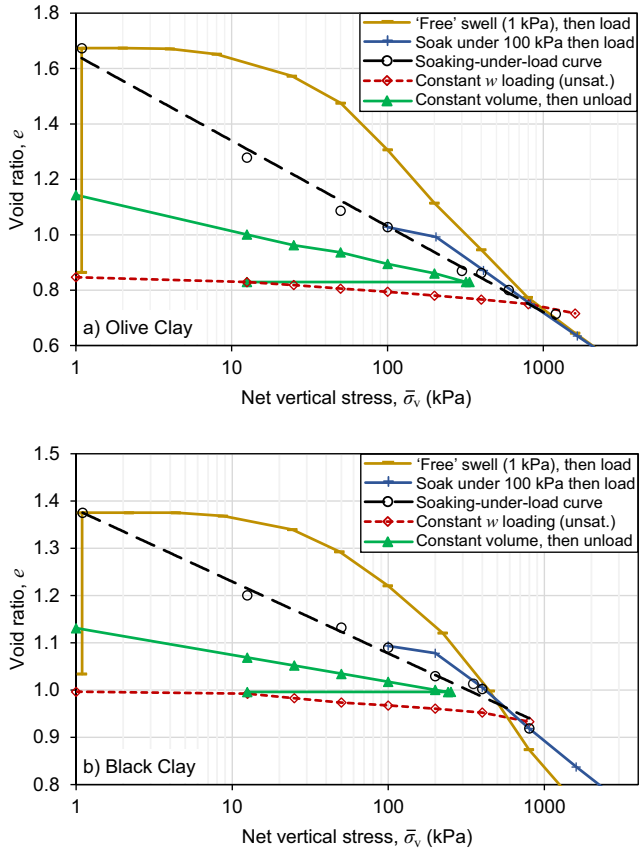

mon point for the Olive Clay, as predicted using the BExM framework. Due to the presence of two sets of NCLs for the Black Clay (as depicted in Fig. 15*b*), this common point may not be as clear in Fig. 21*b*. The curves approximately intersect at a common point when considering the NCL for the 100 kPa test, where destructuring due to the release of strain energy during swelling had likely not occurred.

These experimental results thus suggest that the relationships between the swell pressure and swell potential measured using the various methods can be understood with reference to the BExM framework, for expansive clays with both microfabric type *a* and *b* as defined by Gens and Alonso (1992). It also suggests that regardless of the fabric type, the swell pressure and swell potential recorded using a loading after wetting test soaked under a nominal seating stress are both likely to be greater than the values determined from a soaking-under-load curve from a series of tests at different soaking stresses.

6.9.2. Differences between the two clays and the role of intrinsic properties, initial state, and structure

Any differences in behaviour between the two clays can be attributed to the effects of the intrinsic properties, initial state, soil structure (the combination of bonding and fabric), or some combination of these factors. When considering the characteristics of expansive clays, several studies comparing compacted and intact samples have shown that both the swell potential and swell pressure are independent of soil structure, so long as samples are prepared to the same initial state (Brackley 1983; Armstrong and Zornberg 2017; Gaspar et al. 2022).

To help conceptualise the roles of intrinsic properties and initial state, the authors find it useful to liken an expansive clay to a spring. In this analogy, the stiffness of the spring represents the intrinsic properties of the clay, while the stored potential energy (i.e., the degree to which the spring is compressed) reflects the soil's state.

As indicated previously, intrinsic properties of a soil are those that are independent of state and structure, and depending on the properties of interest, can be determined in various ways. Included in Table 6 and Fig. 16 are key intrinsic parameters as determined for saturated reconstituted specimens subjected to 1D compression and unloading. These results show that the Olive Clay exhibits larger intrinsic compression and expansion indices, indicating a greater susceptibility to volume change under saturated conditions in response to effective stress variations. Meanwhile, the Black Clay's higher smectite content (Table 2) and greater modified free swell index (Table 6) point to a higher potential (intrinsic) expansiveness when exposed to changes in water content under unsaturated conditions.

Despite the greater intrinsic expansiveness of the Black Clay, oedometer tests on compacted samples revealed that the Olive clay displayed a significantly greater swell potential and a higher swell pressure. This seemingly contradictory result can however be explained by revisiting the initial state of the respective samples. Since compacted samples were prepared to reflect the in-situ conditions of the two sites, the initial state (soil suction and void ratio) of the two clays differed. The average initial void ratio for the Olive Clay was lower than that of the Black Clay, both relative to their respective intrinsic void ratios ($e_{0,avg}/e^*_{100} = 0.398$ vs $e_{0,avg}/e^*_{100} = 0.722$), and in numeric value ($e_{0,avg} = 0.853$ vs $e_{0,avg} = 1.003$). Additionally, the initial suction of the Olive Clay was approximately twice as high (5–8 MPa vs 2–4 MPa).

Returning to the spring analogy, the swell tests for the Olive Clay were therefore conducted under a higher initial state of stored potential energy (i.e., a more compressed spring) due to the higher initial suction values and lower initial void ratios. These findings are consistent with those of Brackley (1983), who highlighted that swell pressure is primarily a function of initial void ratio, while swell potential (in void ratio–stress space) is primarily influenced by initial suction. This is also in agreement with the BExM framework (Gens and Alonso 1992), which describes how greater reductions in suction would lead to greater volume increase.

The effects of the different structural arrangements were most notably evident through the two sets of NCLs for the compacted Black Clay, due to the destructuring imposed by large swelling strains, as opposed to the unique NCL for the compacted Olive Clay. The significance of microfabric was also evidenced by collapse upon inundation prior to the onset of swell due to the loss of suction between clay aggregations,

which was only observed for the Olive Clay. Finally, structural effects on a larger scale dictated the time to equilibrium. The continuous network of fissures in Black Clay samples allowed for rapid infiltration of water at lower stresses, allowing for diffusion to take place through a reduced drainage path length and reducing equilibration time. No such continuous fissures were present for the Olive Clay, meaning that the increasing drainage path length for the entire sample due to greater swelling strains at lower stresses caused an increase in equilibration time.

These differences in swelling behaviour highlight the important roles played by state and structure in addition to the intrinsic properties of clays. However, it is noteworthy that despite these differences, the same key trends regarding swell properties obtained using different methods were observed for the two clays with different microstructural arrangements and initial states, and conformance to the BExM framework was evident for both clays as well. This suggests that the same test programme can be followed for the determination of swell properties of a given clay, regardless of the state and structure of the clay being considered.

7. Recommended testing programme

Given the experimental evidence and the interpretation within a critical state soil mechanics-based constitutive model for unsaturated expansive clays, a recommendation on a robust minimum oedometer testing programme for both accurate and conservative estimations of the vertical swell pressure and swell potential can be made. To the authors' knowledge, definitive guidelines on the minimum required tests for these purposes using conventional equipment are not currently available in codes or standards, nor in the literature. The benefit of the implementation of such a programme is that the practitioner can confidently avoid any underestimation of the swell parameters (which may lead to infrastructural damage), whilst avoiding an overly extensive testing programme with too many tests (which would incur unnecessary monetary and lag-time costs).

Brackley (1975) suggested that using only two wetting after loading tests (soaked under 10 and 100 kPa) and plotting a straight line through the points on a semi-log plot was sufficient to estimate swell potential for practical stress ranges. A criticism of this method is that it does not account for soaking-under-load curves with different shapes, such as those reported by Justo et al. (1984) and Al Haj and Standing (2015). Shapes of these curves were previously discussed and although straight lines in semi-log space may generally be valid, more tests would be required to confidently estimate the swell potential even if the relationship is a straight line. Additionally, a test should be conducted where a sample is soaked under a stress high enough to cause compression, so that the swell pressure can be determined using the soaking-under-load curve.

The first facet of the recommended testing programme should be establishing what is required for conservative estimates. Given the previously discussed BExM framework, both the swell pressure and swell potential determined using a loading after wetting test under a small seating stress are greater than or equal to that determined for either of the other two methods (if the NCL for the given sample preparation method is unique). The matter may be more complicated where a unique NCL is not clear, as was observed in this study for the Black Clay.

A soaking-under-load curve should be determined for a more realistic and accurate estimation of swell potential over a range of stresses. This can be done to a sufficient level with significantly fewer tests than conducted in this study. The sample soaked at a low stress will provide the first point on the soaking-under-load curve, and a first estimate of the swell pressure will also be determined from this test. The second test should be conducted at a stress corresponding with the in-situ stress of greatest interest (e.g., overburden stress plus foundation pressure), such that a direct measure of the swell potential for the stress of interest is attained. These first two tests can be conducted simultaneously, since no information from either test is required for the other. The third test should be conducted by soaking a sample under a vertical stress significantly greater than the estimated swell pressure from the first tests (e.g., 1.5–2 times greater, if attainable). This test is guaranteed to result in compression upon soaking, which will provide a point on the soaking-under-load curve that is below the initial void ratio. This provides an estimation of the swell pressure where a curve fitted through the first three points passes through the initial void ratio.

A fourth test is recommended, but not required, and should be conducted at a stress near the swell pressure estimated from the soaking-under-load curve constructed thus far. This would complete the curve and ensure that a reliable estimation of swell pressure is obtained from the soaking-under-load curve. Depending on the coefficient of determination of the best-fit soaking-under-load curve, it may be decided to conduct further tests to complete the curve. The soaking stresses for these tests would depend on the shape of the soaking-under-load curve and where wide gaps exist. It should be emphasised that the high coefficients of determination in the current study and the consistent behaviour between samples was largely due to meticulous experimental procedures and consistent initial conditions, to limit test variability. For a programme such as the one being proposed to be successful, care must be taken to control experimental conditions as far as practically possible. A greater degree of variability between samples would lead to more recommended tests being required.

Each of these wetting after loading tests should also be consolidated to at least the initial void ratio, but preferably to higher stresses such that the uniqueness of the NCL for the given state of structure can be evaluated. This will also give greater confidence that the most conservative swell pressure estimate has been obtained.

Based on the evidence presented in this paper, the first three aforementioned tests and soaking stresses should be sufficient for thorough determination of the swell pressure and swell potential in the majority of cases. The tests listed in this programme also cover both plausible construction sequences, i.e., wetting of the profile before and after placement of the load. It is suggested that a constant volume

Table 8. Proposed testing programme for robust determination of swell properties using a conventional oedometer.

Test No.	Test type	Soaking stress	Required/optional	Comments
1	Wetting after loading, followed by consolidation to high stresses*	"Nominal" e.g., 1, 6, 12.5 kPa	Required	Likely to give the most conservative estimates of both swell pressure and swell potential. This will be the longest test and should commence first
2	Wetting after loading, followed by consolidation to high stresses*	Approximate in-situ stress	Required	Gives a direct measure of swell potential at the in-situ stress. Can be commenced simultaneously with Test 1 or directly afterwards
3	Wetting after loading, followed by consolidation to high stresses*	Twice the swell pressure estimated from Tests 1 and/or 2, or greater	Required	Guarantees compression during inundation, so that swell pressure can be determined from soaking-under-load curve. Test may only commence after one of Tests 1 or 2 (preferably both) has been compressed back to initial volume
4	Wetting after loading, followed by consolidation to high stresses*	Near the swell pressure from Tests 1, 2, and 3	Recommended	Increases the accuracy of the swell pressure from the soaking-under-load curve and the level of detail in the estimated swell potential function. Must commence after the swell phase of Test 3
5	Reconstituted	–	Recommended	Determination of intrinsic properties allows for comparison between soils, or databases such as Burland (1990)
6	Constant water content (unsaturated)	–	Recommended	Allows for the evaluation of volume changes brought about by changes in net stress alone (i.e., loading without changes in water content). Aids interpretation of results within a BExM-based framework (Gens and Alonso 1992) such as in Figs. 5, 6, and 21, or similar
7+	Wetting after loading, followed by consolidation to high stresses*	Dependent on results of Tests 1–4	If necessary, depending on previous tests	Further points on the soaking-under-load curve may be required if the shape is unclear, or if there is significant scatter, non-unique NCLs etc.

*To at least double the stress required to compress the sample back to its initial volume. High enough stresses for convergence onto NCL are preferable.

soaking test is not necessary, since the test significantly underestimates swell potential and does not report a swell pressure of any greater value than those of the previously recommended tests. The test also does not emulate a stress path for any realistic construction sequence, and either requires specialised equipment to conduct or is severely labour-intensive if conventional manual oedometers are used.

If modelling of deformations of the clay due to changes in loading without changes in water content is of interest, then value can be gained from a constant water content test, which is relatively easy to conduct with standard equipment. Such a test would also allow for better understanding of the mechanical responses to wetting and loading through interpretations such as those presented in Figs. 5, 6, and 21. The test is not necessary, however, for the determination of swell properties alone. Another test that is recommended not for swell properties, but as good practice and due to relative ease of testing, is a reconstituted test at an initial water content of 1.0–1.5 times the liquid limit for determination of intrinsic properties as suggested by Burland (1990). This allows for some direct comparisons to be drawn with other clays through their intrinsic properties, independent of structure and stress level. The proposed testing programme is summarised in Table 8.

Figure 22 shows a comparison between the observed swell potential and the predicted swell potential resulting from best-fit logarithmic soaking-under-load curves constructed using: (i) all swell tests, (ii) only "required" tests from Table 8 (Tests 1–3), and (iii) required tests plus the "recommended" swell test from Table 8 (Tests 1–4). Maximum variations in predicted strain ($|\text{Error}|_{\max}$), and the vertical swell pressures ($\bar{\sigma}_{SP,v}$) read off from each soaking-under-load curve, are reported. The two clays tested in this study, as well as results from two comprehensive testing programmes on compacted expansive clays from the literature – the London Clay reported by Monroy et al. (2015) and the El Arahal Clay reported by Justo et al. (1984) – have been plotted. It is evident that the use of only the three "required" tests from Table 8 gives satisfactory results for the prediction of swell properties for all these datasets, with no significant reduction in accuracy. No volumetric strain varies more than 2.3% from the observed result, and the maximum variation in swell pressure for any case is 14%. Adding Test 4 from the "recommended" category does not seem to significantly influence the predicted swell potential, but improves the accuracy of the swell pressure in the majority of cases. The satisfactory accuracy achieved using the recommended testing programme for clays with different microfabrics in this study, as well as two from the literature, gives evidence to support its suitability for any soil fabric.

8. Conclusions

Two highly expansive clays from South Africa, with different geological origins, were characterised in terms of their swell properties using statically compacted oedometer samples. Scanning electron microscope imaging showed that the

Fig. 22. Observed swell potential compared to predictions from soaking-under-load curves determined using all tests or only tests from the testing programme in Table 8: (*a* and *b*) this study; (*c* and *d*) from literature.

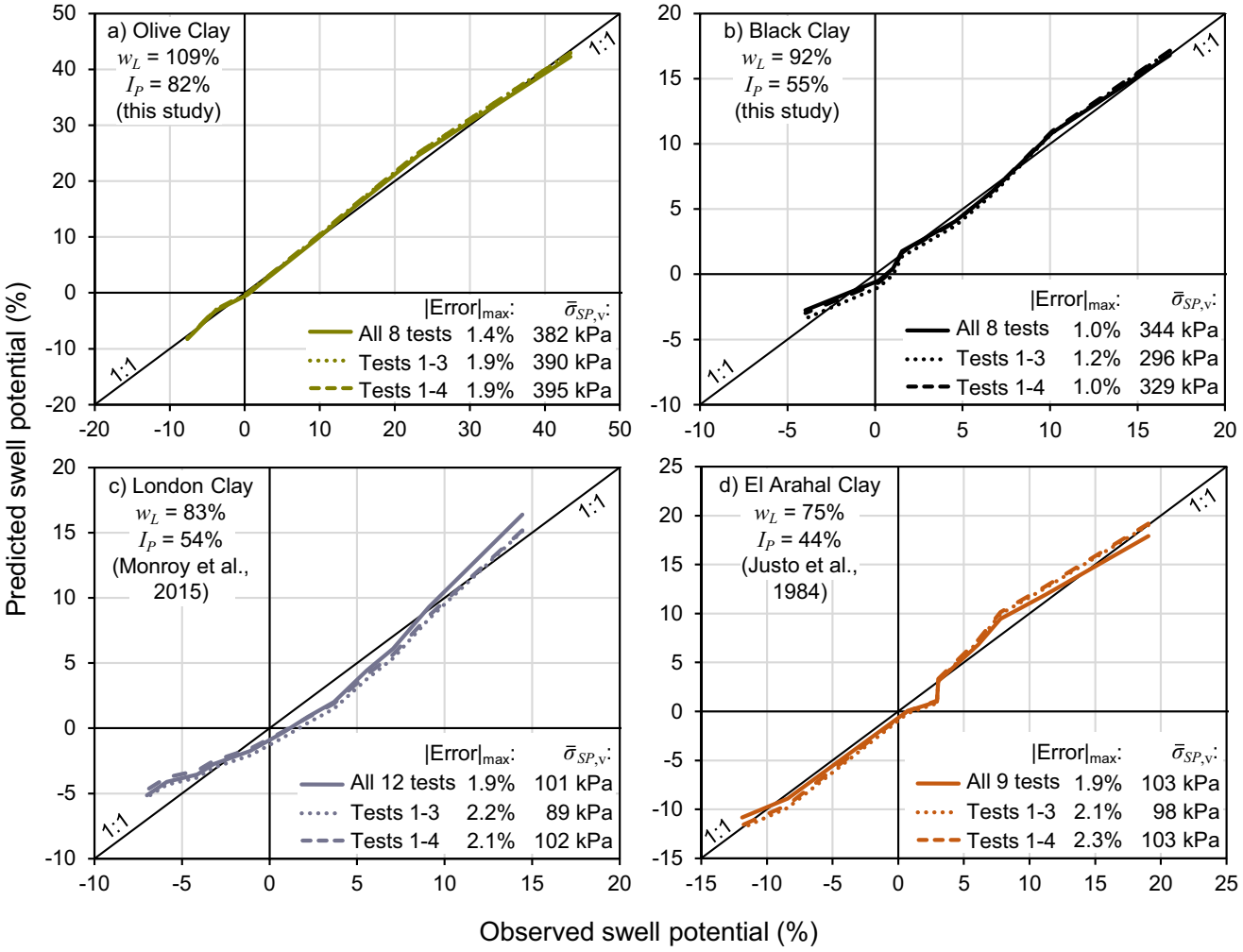

Black Clay was constituted of microfabric type *a* as per Gens and Alonso (1992), with a continuous matrix of elementary clay particles, whereas the Olive Clay contained a microstructural arrangement of aggregations of elementary particles (i.e., type *b*). The influence of the microfabric type was evident through two phenomena. The first was the initial collapse experienced by specimens of the Olive Clay prior to the onset of swell, which was not evident for the Black Clay. This indicated that two separate mechanisms took place upon wetting for the expansive clay with microfabric type *b*, namely (i) macrostructural collapse, followed by (ii) micro- and macrostructural swell. The second phenomenon was the contrasting trends regarding the strain energy release and destructuring imposed during swelling. Destructuring was evident through two sets of NCLs for the Black Clay, where samples subjected to strains of approximately 7% and greater during soaking exhibited a softer response during normal consolidation. In contrast, no evidence of this destructuring due to swell was observed for the Olive Clay, where even samples strained in excess of 40% during soaking converged onto the unique NCL for the given state of structure. This result appears to suggest a more robust structure for the Olive Clay.

Three methods utilising conventional oedometer testing to determine swell pressure and swell potential were compared for each of the clays. For each of the soils, the most conservative estimates of both swell pressure and swell potential were determined from a test following the *loading after wetting* method. Logarithmic soaking-under-load curves (i.e., linear relationships between void ratio and the logarithm of applied stress) were measured for both clays through a series of *wetting after loading* tests. The Barcelona Extended (BExM) framework (Gens and Alonso 1992) was used to conceptually illustrate the stress path-dependency of the swell pressure and swell potential, as well as reasons for variations between the measured properties between the three test methods that were carried out. The experimentally determined swell properties aligned with what was predicted within this framework, regarding the magnitudes recorded using the different test methods relative to one another.

Unloading after constant volume soaking gave the minimum swell potential estimation for both clays. The method

was criticised since it only captures elastic swell, meaning that it is inherently unconservative and not capable of accurately capturing the swell behaviour of a highly expansive clay. Additionally, the constant volume soaking phase is not representative of any typical construction sequence, and reasons are given within the theoretical framework that the swell pressure measured during such a test cannot be the most conservative. This test was thus considered unnecessary for most practical engineering applications.

Given the experimental results and interpretation through a conceptual BExM framework, a testing programme recommended for geotechnical engineering practitioners was proposed for robust determination of the swell pressure and swell potential of a highly expansive clay. The programme consists of a minimum of three swell-under-load tests to utilise both the loading after wetting and wetting after loading methods, with additional optional tests recommended as needed. Using only the required tests yielded satisfactory swell pressure and swell potential predictions for the two clays in this study, as well as London Clay (Monroy et al. 2015) and El Arahal Clay (Justo et al. 1984).

List of symbols

C_c	Compression index
C_c^*	Intrinsic compression index
$C_c(0)$	"Saturated" compression index
$C_c(s)$	Compression index as a function of suction
C_e	Expansion index
C_e^*	Intrinsic expansion index
$C_e(0)$	"Saturated" expansion index
$C_e(s)$	Expansion index as a function of suction
e	Void ratio
e_0	Initial void ratio
$e_{0,avg}$	Average initial void ratio
e_L	Void ratio at the liquid limit
e_{100}^*	Intrinsic void ratio at 100 kPa
e_{1000}^*	Intrinsic void ratio at 1000 kPa
$\lvert\text{Error}\rvert_{\max}$	Maximum error in swell potential prediction
I_P	Plasticity index
$\bar{p}$	Net mean stress
$\bar{p}_0$	Initial net mean stress
$\bar{p}_{in\text{-}situ}$	In-situ net mean stress
$\bar{p}_{SP}$	Swell pressure
$\bar{p}_y$	Yield stress
R^2	Coefficient of determination
s	Suction
s_0	Initial suction
S	Degree of saturation
S_0	Initial degree of saturation
S_{crit}	Critical degree of saturation
u_a	Pore air pressure
u_w	Pore water pressure
V	Volume
V_s	Volume of solids
w	Gravimetric water content
w_0	Initial water content
w_L	Liquid limit
ε_v	Volumetric strain
ε_{vm}	Microstructural volumetric strain
ε_{vM}	Macrostructural volumetric strain
ε_{vM}^P	Plastic macrostructural volumetric strain
$\varepsilon_{v,min}$	Maximum swelling strain
$\varepsilon_v/\varepsilon_{v,min}$	Degree of swell
κ	Slope of non-virgin (elastic) load–unload path
$\kappa(0)$	"Saturated" slope of elastic loading path
$\kappa(s)$	Elastic loading path slope as function of suction
λ	Slope of virgin (elastoplastic) loading path
$\lambda(0)$	"Saturated" slope of virgin loading path (NCL)
$\lambda(s)$	Virgin loading path slope as function of suction
ρ_d	Dry density
σ	Total normal stress
σ'	Effective stress
$\bar{\sigma}$	Net stress
$\bar{\sigma}_{SP,v}$	Vertical swell pressure
σ_v	Vertical total stress
σ_v'	Vertical effective stress
$\bar{\sigma}_v$	Net vertical stress
$\bar{\sigma}_{v,y}$	Vertical yield stress

Acknowledgements

The authors would like to thank the UK Engineering and Physical Sciences Research Council (EPSRC) for funding under the Global Challenges Fund programme for a project entitled "Developing performance-based design for foundations of wind turbines in Africa (WindAfrica)", Grant Ref: EP/P029434/1.

Article information

History dates

Received: 19 October 2024
Accepted: 16 September 2025
Accepted manuscript online: 23 September 2025
Version of record online: 27 November 2025

Data availability

Data will be provided by the corresponding author upon reasonable request.

Author information

Author ORCIDs

R.A. Murison https://orcid.org/0000-0003-0094-2404
T.A.V. Gaspar https://orcid.org/0000-0002-3746-2714
S.W. Jacobsz https://orcid.org/0000-0002-7439-2276
G. Heymann https://orcid.org/0000-0002-2338-4073
A.S. Osman https://orcid.org/0000-0002-5119-8841

Author contributions

Conceptualization: RAM, TAVG, SWJ, GH, ASO
Formal analysis: RAM
Funding acquisition: ASO
Investigation: RAM
Methodology: RAM, TAVG
Project administration: SWJ, ASO
Supervision: TAVG, SWJ, GH
Visualization: RAM, TAVG
Writing – original draft: RAM
Writing – review & editing: TAVG, SWJ, GH, ASO

Competing interests

The authors declare that there are no competing interests which have influenced the content of this article.

Supplementary material

A supplementary document is available with the article at https://doi.org/10.1139/cgj-2024-0642.

References

Al Haj, K.M.A., and Standing, J.R. 2015. Mechanical properties of two expansive clay soils from Sudan. Géotechnique, **65**(4): 258–273. doi:10.1680/geot.14.P.139.

Alonso, E.E., Gens, A., and Josa, A. 1990. A constitutive model for partially saturated soils. Géotechnique, **40**(3): 405–430. doi:10.1680/geot.1990.40.3.405.

Alpan, I. 1957. An apparatus for measuring the swelling pressure in expansive soils. *In* Proceedings of the 4th International Conference on Soil Mechanics and Foundation Engineering, London, August 1957. Vol. 1. Butterworths, London. pp. 1–5.

Armstrong, C.P., and Zornberg, J.G. 2017. Effect of fabric on the swelling characteristics of highly plastic clays. *In* Proceedings 2nd Pan-American Conference on Unsaturated Soils, Dallas, November 2017. ASCE Geotechnical Special Publication 303, Vol. 4. pp. 28–37. doi:10.1061/9780784481707.004.

ASTM. 2021. ASTM D4546-21: Standard Test Methods for One-Dimensional Swell or Collapse of Soils. ASTM International, West Conshohocken. doi:10.1520/D4546-21.

Bagheri, M., Nezhad, M.M., and Rezania, M. 2020. A CRS oedometer cell for unsaturated and non-isothermal tests. Geotechnical Testing Journal, **43**(1): 20–37. doi:10.1520/GTJ20180204.

Baker, R., and Frydman, S. 2009. Unsaturated soil mechanics: critical review of physical foundations. Engineering Geology, **106**(1): 26–39. doi:10.1016/j.enggeo.2009.02.010.

Blight, G.E. 1965. A study of effective stresses for volume change. *In* Moisture equilibria and moisture changes in soils beneath covered areas: a symposium in print. Butterworths, Guildford. pp. 259–269.

Brackley, I.J.A. 1973. Swell pressure and free swell in a compacted clay. *In* Proceedings of the 3rd International Conference on Expansive Soils, Haifa, July 1973. Vol. 1. Jerusalem Academic Press, Jerusalem. pp. 169–176.

Brackley, I.J.A. 1975. Swell under load. *In* Proceedings of the 6th African Regional Conference on Soil Mechanics and Foundation Engineering, Durban, September 1975. Vol. 1. A.A. Balkema, Cape Town. pp. 65–70.

Brackley, I.J.A. 1983. The effects of density, moisture content and loading on swelling of clays. CSIR NBRI Report BOU 66. Council for Scientific and Industrial Research, Pretoria.

BSI. 1990. BS 1377-2:1990. Methods of test for soils for civil engineering purposes – Part 2: Classification tests. British Standards Institution, London.

BSI. 1990. BS 1377-5:1990. Methods of test for soils for civil engineering purposes – Part 5: compressibility, permeability and durability tests. British Standards Institution, London.

BSI. 1999. BS 5930:1999. Code of practice for site investigations. British Standards Institution, London.

Burland, J.B. 1962. The estimation of field effective stresses and the prediction of total heave using a revised method of analysing the double oedometer test. The Civil Engineer in South Africa **4**(6).

Burland, J.B. 1990. On the compressibility and shear strength of natural clays (30th Rankine Lecture). Géotechnique, **40**(3): 329–378. doi:10.1680/geot.1990.40.3.329.

Casagrande, A. 1936. The determination of the pre-consolidation load and its practical significance. *In* Proceedings of the 1st International Conference on Soil Mechanics and Foundation Engineering, Harvard, June 1936. Vol. 3. Geomechanical Engineers Inc., Winchester. pp. 60–64.

Delage, P., and Cui, Y.J. 2008. An evaluation of the osmotic method of controlling suction. Geomechanics and Geoengineering, **3**(1): 1–11. doi:10.1080/17486020701868379.

Delage, P., Howat, M.D., and Cui, Y.J. 1998. The relationship between suction and swelling properties in a heavily compacted unsaturated clay. Engineering Geology, **50**(1–2): 31–48. doi:10.1016/S0013-7952(97)00083-5.

Delage, P., Romero, E., and Tarantino, A. 2008. Recent developments in the techniques of controlling and measuring suction in unsaturated soils. *In* Proceedings of the 1st European Conference on Unsaturated Soils, Durham, July 2008. CRC Press, London. pp. 33–52. doi:10.1201/9780203884430-6.

Dineen, K., and Burland, J.B. 1995. A new approach to osmotically controlled oedometer testing. *In* Proceedings of the 1st International Conference on Unsaturated Soils, Paris, September 1995. Vol. 2. A.A. Balkema, Rotterdam. pp. 459–465.

Fourie, A.B. 1991. Lateral swelling pressure developed in an active clay. *In* Geotechnics in the African Environment – Proceedings of the 10th African Regional Conference on Soil Mechanics and Foundation Engineering and the 3rd International Conference on Tropical and Residual Soils, Maseru, September 1991. Vol. 1. *Edited by* G.E. Blight, A.B. Fourie, I. Luker, D.J. Mouton and R.J. Scheurenberg. A.A. Balkema, Rotterdam. pp. 267–274.

Fredlund, D.G., Hasan, J.U., and Filson, H.L. 1980. The prediction of total heave. *In* Proceedings of the 4th International Conference on Expansive Soils, Denver, June 1980. Vol. 1. ASCE, New York. pp. 1–17.

Gaspar, T.A.V., Jacobsz, S.W., Heymann, G., Toll, D.G., Gens, A., and Osman, A.S. 2022. The mechanical properties of a high plasticity expansive clay. Engineering Geology, **303**: 106647. doi:10.1016/j.enggeo.2022.106647.

Gens, A., and Alonso, E.E. 1992. A framework for the behaviour of unsaturated expansive clays. Canadian Geotechnical Journal, **29**(6): 1013–1032. doi:10.1139/t92-120.

Hilf, J.W. 1956. An investigation of pore-water pressure in compacted cohesive soils. PhD thesis, University of Colorado at Boulder. USBR Technical Memo No. 654. United States Bureau of Reclamation, Denver.

Holtz, W.G., and Gibbs, H.J. 1956. Engineering properties of expansive clays. Transactions of the American Society of Civil Engineers, **121**(1): 641–663. doi:10.1061/TACEAT.0007325.

Jennings, J.E.B., and Burland, J.B. 1962. Limitations to the use of effective stresses in partly saturated soils. Géotechnique, **12**(2): 125–144. doi:10.1680/geot.1962.12.2.125.

Jennings, J.E.B., and Kerrich, J.E. 1962. The heaving of buildings and the associated economic consequences, with particular reference to the Orange Free State Goldfields. The Civil Engineer in South Africa, **4**(11): 221–248. doi:10520/AJA10212019_17314.

Jennings, J.E.B., and Knight, K. 1957. The prediction of total heave from the double oedometer test (Symposium on Expansive Clays, Part I). Transactions of the South African Institution of Civil Engineers, **7**(9): 285–291.

Jennings, J.E.B., Brink, A.B.A., and Williams, A.A.B. 1973b. Revised guide to soil profiling for civil engineering purposes in Southern Africa. The Civil Engineer in South Africa, **15**(1): 3–13. doi:10520/AJA10212019_18390.

Jennings, J.E.B., Firth, R.A., Ralph, T.K., and Nagar, N. 1973a. An improved method for predicting heave using the oedometer test. *In* Proceedings of the 3rd International Conference on Expansive Soils, Haifa, July 1973. Vol. 2. Jerusalem Academic Press, Jerusalem. pp. 149–154.

Jones, D.E., and Holtz, W.G. 1973. Expansive soils: the hidden disaster. ASCE Civil Engineering, **43**(8): 49–51.

Justo, J.L., Delgado, A., and Ruiz, J. 1984. The influence of stress-path in the collapse–swelling of soils at the laboratory. *In* Proceedings of the 5th International Conference on Expansive Soils, Adelaide, May 1984. Institution of Engineers Australia, Barton. pp. 67–71.

Kassiff, G., and Ben Shalom, A. 1971. Experimental relationship between swell pressure and suction. Géotechnique, **21**(3): 245–255. doi:10.1680/geot.1971.21.3.245.

Leroueil, S., and Vaughan, P.R. 1990. The general and congruent effects of structure in natural soils and weak rocks. Géotechnique, **40**(3): 467–488. doi:10.1680/geot.1990.40.3.467.

Likos, W.J., and Lu, N. 2003. Automated humidity system for measuring total suction characteristics of clay. Geotechnical Testing Journal, **26**(2): 179–190. doi:10.1520/GTJ11321J.

Lourenço, S.D.N., Toll, D.G., Augarde, C.E., Gallipoli, D., Congreve, A., Smart, T., and Evans, F.D. 2008. Observations of unsaturated soils by environmental scanning electron microscopy in dynamic mode. *In* Proceedings of the 1st European Conference on Unsaturated Soils, Durham, July 2008. CRC Press, London. pp. 145–150.

Manca, D., Ferrari, A.A.P., and Laloui, L. 2016. Fabric evolution and the related swelling behaviour of a sand/bentonite mixture upon hydro-chemo-mechanical loadings. Géotechnique, **66**(1): 41–57. doi:10.1680/jgeot.15.P.073.

Mantikos, V. 2018. Development of a novel apparatus for establishing swelling and water retention characteristics of bentonite. PhD thesis, Imperial College London. doi:10.25560/87177.

Monroy, R. 2005. The influence of load and suction changes on the volumetric behaviour of compacted London clay. PhD thesis, Imperial College London.

Monroy, R., Ridley, A., Dineen, K., and Zdravković, L. 2007. The suitability of the osmotic technique for the long term testing of partly saturated soils. Geotechnical Testing Journal, **30**(3): 220–226. doi:10.1520/GTJ100731.

Monroy, R., Zdravković, L., and Ridley, A.M. 2015. Mechanical behaviour of unsaturated expansive clay under K_0 conditions. Engineering Geology, **197**: 112–131. doi:10.1016/j.enggeo.2015.08.006.

Murison, R.A., Jacobsz, S.W., Gaspar, T.A.V., da Silva Burke, T.S., and Osman, A.S. 2023. Drying and wetting soil-water retention behaviour of a highly expansive clay under varying initial density. E3S Web of Conferences, **382**: 09005. doi:10.1051/e3sconf/202338209005.

Nelson, J.D., and Miller, D.J. 1992. Expansive soils: Problems and Practice in Foundation and Pavement Engineering. John Wiley & Sons, New York. doi:10.1002/nag.1610171006.

Romero, E., and Simms, P.H. 2008. Microstructure investigation in unsaturated soils: a review with special attention to contribution of mercury intrusion porosimetry and environmental scanning electron microscopy. Geotechnical and Geological Engineering, **26**(6): 705–727. doi:10.1007/s10706-008-9204-5.

Schreiner, H.D. 1988. Volume change of compacted highly plastic African clays. PhD thesis, Imperial College London. doi:10044/1/47643.

Schreiner, H.D., and Burland, J.B. 1991. A comparison of three swell test procedures. *In* Geotechnics in the African Environment – Proceedings of the 10th African Regional Conference on Soil Mechanics and Foundation Engineering and the 3rd International Conference on Tropical and Residual Soils, Maseru, September 1991. Vol 1. *Edited by* G.E. Blight, A.B. Fourie, I. Luker, D.J. Mouton and R.J. Scheurenberg. A.A. Balkema, Rotterdam. pp. 259–266.

Schreiner, H.D., Burland, J.B., and Gourley, C.S. 1994. Swell and collapse of a partially saturated expansive clay. *In* Proceedings of the 13th International Conference on Soil Mechanics and Foundation Engineering, New Delhi, January 1994. Vol. 4. Oxford & IBH Publishing, New Delhi. pp. 1501–1506.

Sivapullaiah, P.V., Sitharam, T.G., and Subba Rao, K.S. 1987. Modified free swell index for clays. Geotechnical Testing Journal, **10**(2): 80–85. doi:10.1520/GTJ10936J.

Skempton, A.W. 1953. The colloidal "activity" of clays. *In* Proceedings of the 3rd International Conference on Soil Mechanics and Foundation Engineering, Zürich, August 1953. Vol. 1. Swiss Society for Soil Mechanics and Foundation Engineering, Zürich. pp. 57–61.

Sridharan, A., Sreepada Rao, A., and Sivapullaiah, P.V. 1986. Swelling pressure of clays. Geotechnical Testing Journal, **9**(1): 24–33. doi:10.1520/GTJ10608J.

Sullivan, R.A., and McClelland, B. 1969. Predicting heave of buildings on unsaturated clay. *In* Proceedings of the 2nd International Conference on Expansive Soils, College Station, August 1969. Texas A&M University Press, College Station. pp. 404–420.

Tarantino, A., and Mongiovi, L. 2000. A study of the efficiency of semi-permeable membranes in controlling soil matrix suction using the osmotic technique. *In* Unsaturated Soils for Asia. *Edited by* H. Rahardjo, D.G. Toll and E.C. Leong. CRC Press, London. pp. 303–308. doi:10.1201/9781003078616-50.

Terzaghi, K. von. 1936. The shearing resistance of saturated soils and the angle between the planes of shear. *In* Proceedings of the 1st International Conference on Soil Mechanics and Foundation Engineering, Harvard, June 1936. Vol. 1. Geomechanical Engineers Inc., Winchester. pp. 54–56.

Thomson, W. 1871. On the equilibrium of vapour at a curved surface of liquid. The London, Edinburgh, and Dublin Philosophical Magazine and Journal of Science, **42**(282): 448–452. doi:10.1080/14786447108640606.

Van der Merwe, D.H. 1975. Plasticity index and percentage clay fraction of soils – in speciality session B: current theory and practice in building on expansive clays. *In* Proceedings of the 6th African Regional Conference on Soil Mechanics and Foundation Engineering, Durban, September 1975. Vol. 2. A.A. Balkema, Cape Town. pp. 166–167.

Williams, A.A.B., Pidgeon, J.T., and Day, P.W. 1985. Expansive soils. Problem soils in South Africa – state of the art. The Civil Engineer in South Africa, **27**(7): 367–377. doi:10520/EJC24998.